

# Diagnostics for Monte Carlo Algorithms for Models with Intractable Normalising Functions

Bokgyeong Kang<sup>1</sup>, John Hughes<sup>2</sup>, and Murali Haran<sup>1</sup>

<sup>1</sup>Department of Statistics, Pennsylvania State University

<sup>2</sup>College of Health, Lehigh University

## Abstract

Models with intractable normalising functions have numerous applications ranging from network models and image analysis to models for count data. Because the normalising constants are functions of the parameters of interest, standard Markov chain Monte Carlo cannot be used for Bayesian inference for these models. A number of algorithms have been developed for such models. Some have the posterior distribution as the asymptotic distribution. Other “asymptotically inexact” algorithms do not possess this property. There is limited guidance for evaluating approximations based on these algorithms, and hence it is very hard to tune them. We propose two new diagnostics that address these problems for intractable normalising function models. Our first diagnostic, inspired by the second Bartlett identity, is, in principle, applicable in most any likelihood-based context where misspecification is of concern. We develop an approximate version that is applicable to intractable normalising function problems. Our second diagnostic is a Monte Carlo approximation to a kernel Stein discrepancy-based diagnostic introduced by Gorham and Mackey (2017). We provide theoretical justification for our methods and apply them to several algorithms in the context of challenging simulated and real data examples including an Ising model, an exponential random graph model, and a Conway–Maxwell–Poisson regression model.

*Keywords:* Bartlett identity, doubly intractable distributions, kernel Stein discrepancy, Markov chain Monte Carlo, sample quality measure, Ising model

# 1 Introduction

Models with intractable normalising functions arise in many contexts, notably the Ising (Lenz, 1920; Ising, 1925) and autologistic models (see Besag, 1974; Hughes et al., 2011, for a review) for binary data on a lattice, exponential random graph models (see Robins et al., 2007; Hunter and Handcock, 2006) and mixed graphical models (see Lauritzen and Wermuth, 1989; Lee and Hastie, 2015; Cheng et al., 2017) for explaining relationships among actors in networks, interaction point process models (see Strauss, 1975; Goldstein et al., 2015) for describing spatial patterns among points, and Conway–Maxwell–Poisson regression models (see Conway and Maxwell, 1962; Shmueli et al., 2005; Chanialidis et al., 2018) for over- or under-dispersed count data. Standard Markov chain Monte Carlo (MCMC) algorithms cannot be applied to these models. Suppose that we have data  $\mathbf{x} \in \mathcal{X}$  generated from a probability model with likelihood function  $L(\boldsymbol{\theta} \mid \mathbf{x}) = h(\mathbf{x} \mid \boldsymbol{\theta})/c(\boldsymbol{\theta})$ , where  $c(\boldsymbol{\theta})$  is a normalising function, and a prior density  $p(\boldsymbol{\theta})$ . The posterior density of  $\boldsymbol{\theta}$  is

$$\pi(\boldsymbol{\theta} \mid \mathbf{x}) \propto p(\boldsymbol{\theta}) \frac{h(\mathbf{x} \mid \boldsymbol{\theta})}{c(\boldsymbol{\theta})},$$

which brings about so-called doubly intractable posterior distributions. A major problem in constructing a standard MCMC algorithm for such models is that  $c(\boldsymbol{\theta})$  cannot be easily evaluated. The Metropolis–Hastings (MH) algorithm (Metropolis et al., 1953; Hastings, 1970) acceptance probability at each step requires evaluating the unknown ratio  $c(\boldsymbol{\theta})/c(\boldsymbol{\theta}')$ , where  $\boldsymbol{\theta}'$  denotes the proposed value.

A wide range of computational methods have been proposed for Bayesian inference for doubly intractable posterior distributions (see Park and Haran, 2018, for a review). There are asymptotically exact algorithms whose Markov chain has a stationary distribution equal to its target distribution (Møller et al., 2006; Murray et al., 2006; Atchadé et al., 2013; Lyne et al., 2015; Liang et al., 2016). Throughout this manuscript we use “target distribution” to refer to the posterior distribution of interest. The algorithms of Møller et al. (2006) and Murray et al. (2006) require the ability to generate samples exactly from the probability model, which is available only for a small class of probability models having

intractable normalising functions. The other asymptotically exact algorithms do not need exact sampling but are complicated to construct and have to be carefully tuned to provide reliable inference. These algorithms tend to be computationally intensive (Park and Haran, 2018). There are asymptotically inexact algorithms that may be much faster and can be applied to a wider class of problems (Liang, 2010; Alquier et al., 2016; Park and Haran, 2020). An asymptotically inexact algorithm either converges to an approximation of the target or is not known to converge to any distribution. The performance of these algorithms relies on the choice of various tuning parameters. It is also not always easy to judge the tradeoffs between using a faster asymptotically inexact algorithm and a potentially more computationally expensive but asymptotically exact algorithm. Hence, it is crucial to have diagnostics that provide guidance for users to carefully tune their algorithms to provide reliable results.

There is a large literature on convergence diagnostics for MCMC algorithms (see Cowles and Carlin, 1996; Flegal and Jones, 2011; Roy, 2020, for reviews). However, the literature on assessing the quality of approximations provided by asymptotically inexact algorithms is rather limited. Fan et al. (2006), Gorham and Mackey (2015), and Gorham and Mackey (2017) have proposed diagnostics that measure the deviation between sample means and target expectations whose values are known. The approaches by Gorham and Mackey (2015) and Gorham and Mackey (2017) are supported by theories of weak convergence. Lee et al. (2019) and Xing et al. (2019) have provided tools for assessing the coverage of approximate credible intervals. These are laudable innovations, but they are not available for asymptotically inexact algorithms for doubly intractable distributions. This motivates the development of diagnostic tools that assist scientists in tuning these algorithms. Following Gorham and Mackey (2017), we think of our diagnostics as measuring “sample quality.”

In this article we describe a new diagnostic method that uses the well known second Bartlett identity (cf. Bartlett, 1953a,b). Our method is, in principle, applicable in most any likelihood-based context where misspecification is of concern. We develop a Monte Carlo approximation to this new diagnostic that is applicable to intractable normalising function models. We also develop an approximate version of the kernel Stein discrepancy

introduced by Gorham and Mackey (2017), making this available for doubly intractable distributions. This diagnostic asymptotically inherits the same convergence properties as that of Gorham and Mackey (2017) and thus can be used for diagnosing convergence of a sequence of sample distributions to the target distribution.

The remainder of this article is organised as follows. In Section 2 we briefly describe computational methods for models with intractable normalising functions. In Section 3 we discuss the need for diagnostics for tuning asymptotically inexact algorithms. In Section 4 we propose a new diagnostic for asymptotically exact and inexact methods, and we develop an approximation for doubly intractable distributions. In Section 5 we briefly describe the kernel Stein discrepancy introduced by Gorham and Mackey (2017) and propose its Monte Carlo approximation for intractable normalising function models. We provide theoretical justification for our diagnostics. In Section 6 we describe the application of our diagnostic approaches to several algorithms in the context of three different challenging examples and study the computational complexity and variability of our diagnostics. Finally, in Section 7 we conclude with a brief summary and discussion.

## 2 Inference for models with intractable normalising functions

Several computational methods have been developed for Bayesian inference for models with intractable normalising functions. Park and Haran (2018) categorised these algorithms into two general, overlapping classes: (1) *auxiliary variable approaches*, which introduce an auxiliary variable and cancel out the normalising functions in the Metropolis–Hastings acceptance probability (Møller et al., 2006; Murray et al., 2006; Liang, 2010; Liang et al., 2016), and (2) *likelihood approximation approaches*, which directly approximate the normalising functions and plug the approximations into the Metropolis–Hastings acceptance probability (Atchadé et al., 2013; Lyne et al., 2015; Alquier et al., 2016; Park and Haran, 2020). An important characteristic of these algorithms is whether they are “asymptotically exact” or “asymptotically inexact.” Consider a weighted sample defined as  $Q_n = \sum_{i=1}^n q_n(\boldsymbol{\theta}^{(i)})\delta_{\boldsymbol{\theta}^{(i)}}$

with sample  $\boldsymbol{\theta}^{(1)}, \dots, \boldsymbol{\theta}^{(n)}$ , probability mass function  $q_n$ , and weights  $\delta$ . We use “asymptotic distribution of the sample” to represent the limiting distribution of the sequence of sample distributions  $Q_n$ . Asymptotically exact algorithms generate samples whose asymptotic distribution is exactly equal to the target distribution. Asymptotically inexact algorithms generate samples that do not converge to the target distribution (or to any distribution in some cases).

Asymptotically exact algorithms have attractive theoretical properties but can often be computationally burdensome or even infeasible for challenging models. For instance, Møller et al. (2006) and Murray et al. (2006) depend on perfect sampling (cf. Propp and Wilson, 1996), an algorithm that generates an auxiliary variable exactly from the target distribution using bounding Markov chains. Perfect samplers tend to be very computationally expensive and are available only for a small class of probability models. Atchadé et al. (2013) and Liang et al. (2016) propose asymptotically exact algorithms that do not need perfect sampling. These algorithms require storing simulated auxiliary data or its sufficient statistics with each iteration. The computational and memory costs are very expensive for models without low-dimensional sufficient statistics. Pseudo-marginal MCMC algorithms (Beaumont, 2003; Andrieu and Roberts, 2009) are approaches that use an unbiased Monte Carlo approximation of an intractable likelihood. And Lyne et al. (2015) constructed an unbiased likelihood estimate for models with intractable normalising functions. To obtain a single estimate, their approach requires multiple Monte Carlo approximations to the normalising constant and thus can often be computationally prohibitive.

Several computationally efficient asymptotically inexact algorithms have also been proposed. For instance, the double Metropolis–Hastings (DMH) sampler, proposed by Liang (2010), replaces perfect sampling with a standard Metropolis–Hastings algorithm, an “inner sampler,” at each iteration. The DMH algorithm is easy to implement and is computationally efficient compared to the other algorithms discussed thus far. But the inner sampling becomes more computationally expensive with an increase in the dimension of the data. For large data problems, Park and Haran (2020) proposed a function emulation algorithm that approximates the likelihood normalising function (or full likelihood function) at several

parameter values and interpolates the function using a Gaussian process. This provides significant gains in computational efficiency.

Both asymptotically exact and inexact algorithms require careful tuning in order to provide good approximations in a reasonable amount of time. For instance, the DMH algorithm requires users to decide the length  $m$  of the inner sampler for generating an auxiliary variable. As  $m$  grows large the auxiliary variable becomes approximately a draw from the probability model at the expense of longer computing time. The function emulation algorithm requires users to select (1) an appropriate number of particles to cover the important region of the parameter space, and (2) the sample size for approximating the likelihood normalising function (or full likelihood function) at each particle. However, currently there is little guidance on how to tune these algorithms, and most of them rely on simulation studies. Also, the behavior of the algorithm varies across models or across datasets for a given model.

### 3 The need for diagnostics for intractable normalising function problems

There is a vast literature on MCMC convergence diagnostics (see Cowles and Carlin, 1996; Flegal and Jones, 2011; Roy, 2020, for reviews). However, these diagnostics may not be adequate for asymptotically inexact algorithms. Suppose we have a sample generated by an asymptotically inexact method. Such a sample may not have an asymptotic distribution, or said sample may converge but to a mere approximation of the target distribution. Standard MCMC diagnostics assess whether the sample has converged to its asymptotic distribution but do not assess whether the asymptotic distribution is equal to the target distribution. As discussed in Section 2, however, asymptotically exact algorithms for models with intractable normalising functions are available only for a few special cases, and even for these cases computing tends to be quite burdensome.

A number of approaches based on measuring the difference between sample means and target expectations have been proposed for assessing the quality of approximations provided

by asymptotically inexact algorithms. Fan et al. (2006) proposed score function diagnostics for assessing estimates of some quantities the values of which are known under the target distribution. They suggested plotting the Monte Carlo estimate versus the sample size together with error bounds. Gorham and Mackey (2015) pointed out limitations of the score function diagnostics caused by considering only a finite class of functions and introduced a new diagnostic method based on a Stein discrepancy. Gorham and Mackey (2015) defined Stein discrepancies that bound the discrepancy between the sample mean and the target expectation over a large collection of functions whose target expectations are zero. The Stein discrepancies are supported by a theory of weak convergence and are attainable by solving a linear program. Combining this idea with the theory of reproducing kernels, Gorham and Mackey (2017) provided a closed-form kernel Stein discrepancy with sound theoretical support analogous to that of Gorham and Mackey (2015) (see Section 5.1 for details). These approaches are useful for comparing asymptotically approximate samplers and for selecting tuning parameters for such samplers. However, all of them require evaluating the score function of the target density, which is not possible for doubly intractable posterior distributions. In contrast, our approaches apply broadly to asymptotically exact and inexact algorithms even for such challenging problems. To our knowledge, no other diagnostics are currently available for asymptotically inexact algorithms for models with intractable normalising functions. We have studied our diagnostics as applied in several challenging real data settings. In addition, we are able to provide some theoretical justification for our methods.

## 4 Curvature diagnostic

In this section we introduce two new diagnostics that are useful for tuning asymptotically exact and inexact algorithms: a curvature diagnostic (CD) and an approximate curvature diagnostic (ACD). The curvature diagnostic is based on the second Bartlett identity from the classical theory of maximum likelihood. The approximate curvature diagnostic is an approximation of the CD that is suitable for intractable normalising function problems.

## 4.1 A general purpose curvature diagnostic

Consider a sequence of sample points  $\boldsymbol{\theta}^{(1)}, \dots, \boldsymbol{\theta}^{(n)}$  generated by an algorithm having  $\pi(\boldsymbol{\theta} \mid \mathbf{x})$  as its target distribution. Our aim is to determine whether the sample will produce a good approximation to some quantity of interest, e.g.,  $E_\pi\{z(\boldsymbol{\theta})\}$ . One possible approach is to use functions whose expectations are known under the target distribution. One such function is the score function, which has expectation zero by the first Bartlett identity. Based on this, Fan et al. (2006) proposed the score function diagnostic described in Section 3. Our diagnostic, the curvature diagnostic, is inspired by the method for obtaining the asymptotic variance of a maximum likelihood estimator under a misspecified model. When the model is misspecified, the second Bartlett identity does not hold, which is to say (see details below) the sensitivity matrix is not equal to the variability matrix. And so the asymptotic variance of the estimator does not simplify to the inverse of the Fisher information. Our curvature diagnostic uses the dissimilarity between the sensitivity matrix and the variability matrix to assess the quality of the sample. We provide details in the following paragraph.

Let  $\mathbf{u}(\boldsymbol{\theta}) = \nabla_{\boldsymbol{\theta}} \log \pi(\boldsymbol{\theta} \mid \mathbf{x})$  be the score function of the posterior density  $\pi(\boldsymbol{\theta} \mid \mathbf{x})$ . The posterior density has the sensitivity matrix

$$E_\pi \left\{ -\frac{\partial}{\partial \boldsymbol{\theta}} \mathbf{u}(\boldsymbol{\theta}) \right\} = \int_{\Theta} -\frac{\partial}{\partial \boldsymbol{\theta}} \mathbf{u}(\boldsymbol{\theta}) \pi(\boldsymbol{\theta} \mid \mathbf{x}) d\boldsymbol{\theta}$$

and the variability matrix

$$\text{var}_\pi \{ \mathbf{u}(\boldsymbol{\theta}) \} = E_\pi \{ \mathbf{u}(\boldsymbol{\theta}) \mathbf{u}(\boldsymbol{\theta})^\top \}. \quad (1)$$

The second equation of (1) follows from Bartlett's first identity:  $E_\pi\{\mathbf{u}(\boldsymbol{\theta})\} = \mathbf{0}$ . Let  $H(\boldsymbol{\theta}) = \frac{\partial}{\partial \boldsymbol{\theta}} \mathbf{u}(\boldsymbol{\theta})$ ,  $J(\boldsymbol{\theta}) = \mathbf{u}(\boldsymbol{\theta}) \mathbf{u}(\boldsymbol{\theta})^\top$ , and  $\mathbf{d}(\boldsymbol{\theta}) = \text{vech}[J(\boldsymbol{\theta}) + H(\boldsymbol{\theta})]$ , where  $\text{vech}(M)$  denotes the half-vectorisation of the matrix  $M$ . We have  $E_\pi\{\mathbf{d}(\boldsymbol{\theta})\} = \mathbf{0}$  by Bartlett's second identity:  $E_\pi\{-H(\boldsymbol{\theta})\} = E_\pi\{J(\boldsymbol{\theta})\}$ . Using the sample  $\boldsymbol{\theta}^{(1)}, \dots, \boldsymbol{\theta}^{(n)}$  we construct a Monte Carlo approximation to the half-vectorised difference between the sensitivity and

variability matrices as

$$\bar{\mathbf{d}}_n := \frac{1}{n} \sum_{i=1}^n \mathbf{d}(\boldsymbol{\theta}^{(i)}). \quad (2)$$

Suppose that the samples  $\boldsymbol{\theta}^{(1)}, \dots, \boldsymbol{\theta}^{(n)}$  are independent. By the central limit theorem, we have

$$\sqrt{n} \bar{\mathbf{d}}_n \xrightarrow{d} \mathcal{N}(\mathbf{0}, V),$$

where  $V := \text{cov}_\pi[\mathbf{d}(\boldsymbol{\theta})] = \mathbb{E}_\pi [\mathbf{d}(\boldsymbol{\theta}) \mathbf{d}(\boldsymbol{\theta})^\top]$ . Our unbiased and consistent approximation of  $V$  is calculated as

$$\hat{V}_n := \frac{1}{n} \sum_{i=1}^n \mathbf{d}(\boldsymbol{\theta}^{(i)}) \mathbf{d}(\boldsymbol{\theta}^{(i)})^\top. \quad (3)$$

Our curvature diagnostic is then defined as follows.

**Definition 1 (Curvature Diagnostic (CD))** Consider an i.i.d. sample  $\boldsymbol{\theta}^{(1)}, \dots, \boldsymbol{\theta}^{(n)}$  generated by an algorithm having  $\pi(\boldsymbol{\theta} \mid \mathbf{x})$  as its target. Let  $\bar{\mathbf{d}}_n$  be a Monte Carlo approximation, computed using the sample, to the half-vectorised difference between the sensitivity and variability matrices of the target density. Let  $\hat{V}_n$  be a Monte Carlo approximation, computed with the sample, to the asymptotic covariance matrix of  $\bar{\mathbf{d}}_n$ . Our curvature diagnostic is defined as

$$\mathcal{C}_n(\mathbf{x}) := n \bar{\mathbf{d}}_n^\top \hat{V}_n^{-1} \bar{\mathbf{d}}_n,$$

and  $\mathcal{C}_n(\mathbf{x})$  has an asymptotic  $\chi^2(r)$  distribution, where  $r$  is the dimension of  $\bar{\mathbf{d}}_n$ , if the asymptotic distribution of the sample is equal to the target distribution.

A simple and effective heuristic for determining  $n$  is to plot  $\hat{V}_n$  against the posterior sample size  $n$  and select  $n$  at which the approximation appears to have stabilised. Given  $n$ , we reject the null hypothesis that the asymptotic distribution of the sample is equal to the target distribution if  $\mathcal{C}_n(\mathbf{x})$  is greater than the  $1 - \alpha$  quantile of the  $\chi^2(r)$  distribution,

where  $\alpha$  is the significance level. We found that  $\alpha = 0.01$  performed well in our simulation experiments, and so we take  $\alpha = 0.01$  in the sequel.

If  $\boldsymbol{\theta}^{(1)}, \dots, \boldsymbol{\theta}^{(n)}$  are from a Markov process and thus dependent, we may thin the samples such that auto-correlation is sufficiently reduced. This might require generating very long sample paths when parameters are strongly correlated. Alternatively we may use the asymptotic normality of Markov chain Monte Carlo estimators. By the Markov chain central limit theorem  $\sqrt{n}\bar{\mathbf{d}}_n$  is asymptotically normally distributed and the asymptotic covariance matrix can be estimated by the batch means method. The batch means estimator is strongly consistent under some conditions (Damerdji, 1994; Jones et al., 2006). Because it is simple to construct and appears to work well in practice under quite a wide range of settings (cf. Flegal et al., 2008), we suggest using batch means.

## 4.2 An approximate curvature diagnostic for intractable normalising function problems

If the normalising function  $c(\boldsymbol{\theta})$  of the likelihood is intractable, it is not possible to evaluate the curvature diagnostic since the diagnostic involves  $\nabla_{\boldsymbol{\theta}} \log c(\boldsymbol{\theta})$ ,  $\{\nabla_{\boldsymbol{\theta}} \log c(\boldsymbol{\theta})\} \{\nabla_{\boldsymbol{\theta}} \log c(\boldsymbol{\theta})\}^\top$ , and  $\frac{\partial}{\partial \boldsymbol{\theta}} \nabla_{\boldsymbol{\theta}} \log c(\boldsymbol{\theta})$ . We therefore employ Monte Carlo approximations. To do this, we write the  $k$ th entry of the vector  $\nabla_{\boldsymbol{\theta}} \log c(\boldsymbol{\theta})$  as an expectation with respect to the model distribution:

$$\frac{\partial \log c(\boldsymbol{\theta})}{\partial \theta_k} = \mathbb{E}_f \left\{ \frac{\partial \log h(\mathbf{X} | \boldsymbol{\theta})}{\partial \theta_k} \right\}, \quad k = 1, \dots, p. \quad (4)$$

The derivation of (4) can be found in the supplementary materials. We approximate (4) using a sample generated from the model distribution:

$$\frac{\partial \log c(\boldsymbol{\theta})}{\partial \theta_k} \approx \frac{1}{N} \sum_{j=1}^N \frac{\partial \log h(\mathbf{y}^{(j)} | \boldsymbol{\theta})}{\partial \theta_k}, \quad (5)$$

where  $\mathbf{y}^{(1)}, \dots, \mathbf{y}^{(N)}$  are auxiliary variables generated exactly from  $f(\cdot | \boldsymbol{\theta})$  or generated by a Monte Carlo algorithm having  $f(\cdot | \boldsymbol{\theta})$  as its target distribution. In a similar fashion, the

approximation of the  $(k, l)$ th entry of  $\{\nabla_{\boldsymbol{\theta}} \log c(\boldsymbol{\theta})\} \{\nabla_{\boldsymbol{\theta}} \log c(\boldsymbol{\theta})\}^\top$  is calculated as

$$\frac{\partial \log c(\boldsymbol{\theta})}{\partial \theta_k} \frac{\partial \log c(\boldsymbol{\theta})}{\partial \theta_l} \approx \left\{ \frac{1}{N} \sum_{j=1}^N \frac{\partial \log h(\mathbf{y}^{(j)} | \boldsymbol{\theta})}{\partial \theta_k} \right\} \left\{ \frac{1}{N} \sum_{j=1}^N \frac{\partial \log h(\mathbf{y}^{(j)} | \boldsymbol{\theta})}{\partial \theta_l} \right\}, \quad k, l = 1, \dots, p.$$

Finally, to approximate  $\frac{\partial}{\partial \boldsymbol{\theta}} \nabla_{\boldsymbol{\theta}} \log c(\boldsymbol{\theta})$  we write its  $(k, l)$ th entry as an expectation with respect to the model distribution:

$$\begin{aligned} \frac{\partial^2 \log c(\boldsymbol{\theta})}{\partial \theta_k \partial \theta_l} &= \mathbb{E}_f \left\{ \frac{\partial^2 \log h(\mathbf{X} | \boldsymbol{\theta})}{\partial \theta_k \partial \theta_l} \right\} + \mathbb{E}_f \left\{ \frac{\partial \log h(\mathbf{X} | \boldsymbol{\theta})}{\partial \theta_k} \frac{\partial \log h(\mathbf{X} | \boldsymbol{\theta})}{\partial \theta_l} \right\} \\ &\quad - \mathbb{E}_f \left\{ \frac{\partial \log h(\mathbf{X} | \boldsymbol{\theta})}{\partial \theta_k} \right\} \mathbb{E}_f \left\{ \frac{\partial \log h(\mathbf{X} | \boldsymbol{\theta})}{\partial \theta_l} \right\}. \end{aligned} \quad (6)$$

The derivation of (6) can be found in the supplementary materials. This leads to the approximation

$$\begin{aligned} \frac{\partial^2 \log c(\boldsymbol{\theta})}{\partial \theta_k \partial \theta_l} &\approx \frac{1}{N} \sum_{j=1}^N \frac{\partial^2 \log h(\mathbf{y}^{(j)} | \boldsymbol{\theta})}{\partial \theta_k \partial \theta_l} + \frac{1}{N} \sum_{j=1}^N \frac{\partial \log h(\mathbf{y}^{(j)} | \boldsymbol{\theta})}{\partial \theta_k} \frac{\partial \log h(\mathbf{y}^{(j)} | \boldsymbol{\theta})}{\partial \theta_l} \\ &\quad - \left\{ \frac{1}{N} \sum_{j=1}^N \frac{\partial \log h(\mathbf{y}^{(j)} | \boldsymbol{\theta})}{\partial \theta_k} \right\} \left\{ \frac{1}{N} \sum_{j=1}^N \frac{\partial \log h(\mathbf{y}^{(j)} | \boldsymbol{\theta})}{\partial \theta_l} \right\}. \end{aligned}$$

By plugging these approximations into  $\mathbf{d}(\boldsymbol{\theta})$ , we obtain its approximation  $\hat{\mathbf{d}}_N(\boldsymbol{\theta})$ . By replacing  $\mathbf{d}(\boldsymbol{\theta})$  with its approximation  $\hat{\mathbf{d}}_N(\boldsymbol{\theta})$  in (2) and (3), we obtain a Monte Carlo approximation  $\hat{\mathbf{d}}_{n,N}$  to  $\bar{\mathbf{d}}_n$  and a second-stage approximation  $\hat{V}_{n,N}$  to the asymptotic covariance matrix of  $\bar{\mathbf{d}}_n$ . Then an approximate version of the curvature diagnostic for intractable normalising function problems can be defined as follows.

**Definition 2 (Approximate Curvature Diagnostic (ACD))** Consider an i.i.d. sample  $\boldsymbol{\theta}^{(1)}, \dots, \boldsymbol{\theta}^{(n)}$  generated by an algorithm having  $\pi(\boldsymbol{\theta} | \mathbf{x})$  as its target. Consider auxiliary variables  $\mathbf{y}^{(1)}, \dots, \mathbf{y}^{(N)}$  generated from the model distribution. Let  $\bar{\mathbf{d}}_n$  be the sample mean of half-vectorised difference between the sensitivity and variability matrices of the target density and  $\hat{\mathbf{d}}_{n,N}$  be a Monte Carlo approximation, computed using the sample and auxiliary variables, to  $\bar{\mathbf{d}}_n$ . Let  $\hat{V}_{n,N}$  be a two-stage Monte Carlo approximation, computed using the sample and auxiliary variables, to the asymptotic covariance matrix of  $\bar{\mathbf{d}}_n$ . Our approximate

curvature diagnostic is defined as

$$\hat{\mathcal{C}}_{n,N}(\mathbf{x}) := n \hat{\mathbf{d}}_{n,N}^\top \hat{V}_{n,N}^{-1} \hat{\mathbf{d}}_{n,N}.$$

To provide theoretical justification for this diagnostic, we make the following assumptions regarding the prior density  $p(\boldsymbol{\theta})$  and the unnormalised probability model density  $h(\mathbf{x} \mid \boldsymbol{\theta})$ . We use  $\|\cdot\|_{\max}$  to represent the max norm of vectors or matrices.

**Assumption 1** *There exist constants  $c'_p$  and  $c''_p$  such that  $\|\nabla_{\boldsymbol{\theta}} \log p(\boldsymbol{\theta})\|_{\max} \leq c'_p$  and  $\|\frac{\partial}{\partial \boldsymbol{\theta}} \nabla_{\boldsymbol{\theta}} \log p(\boldsymbol{\theta})\|_{\max} \leq c''_p$ .*

**Assumption 2** *There exist constants  $c'_h$  and  $c''_h$  such that  $\|\nabla_{\boldsymbol{\theta}} \log h(\mathbf{x} \mid \boldsymbol{\theta})\|_{\max} \leq c'_h$  and  $\|\frac{\partial}{\partial \boldsymbol{\theta}} \nabla_{\boldsymbol{\theta}} \log h(\mathbf{x} \mid \boldsymbol{\theta})\|_{\max} \leq c''_h$ .*

Since the prior density is determined by the user, the prior's score function and Hessian matrix may be assumed to be bounded. In many applications Assumption 2 may be checked easily. In particular, Assumption 2 is satisfied with high probability for exponential families. For a probability model in an exponential family, the model's score is its summary statistics and the first inequality of Assumption 2 is satisfied with high probability (Chazottes et al., 2007). The model's Hessian matrix is zero and the second inequality is satisfied almost surely. Under these assumptions, Theorem 1 quantifies the distance between the asymptotic covariance matrix  $V$  and its two-stage approximation  $\hat{V}_{n,N}$ .

**Theorem 1** *Consider an i.i.d. sample  $\boldsymbol{\theta}^{(1)}, \dots, \boldsymbol{\theta}^{(n)}$  generated by an algorithm having  $\pi(\boldsymbol{\theta} \mid \mathbf{x})$  as its target. Suppose Assumptions 1 and 2 hold. If the asymptotic distribution of the sample is equal to the target distribution, we have*

$$\|\hat{V}_{n,N} - V\|_{\max} = \left\| \frac{1}{n} \sum_{i=1}^n \hat{\mathbf{d}}_N(\boldsymbol{\theta}^{(i)}) \hat{\mathbf{d}}_N(\boldsymbol{\theta}^{(i)})^\top - \mathbb{E}_\pi[\mathbf{d}(\boldsymbol{\theta}) \mathbf{d}(\boldsymbol{\theta})^\top] \right\|_{\max} \leq \delta(n) + g(c'_p, c'_h, c''_p, c''_h) \epsilon(N)$$

almost surely for some bounded function  $g$ ,  $\delta(n) = \mathcal{O}(1/\sqrt{n})$ , and  $\epsilon(N) = \mathcal{O}(1/\sqrt{N})$ .

A proof of Theorem 1 and the function  $g$  are provided in the supplementary materials. Provided the theorem holds, the two-stage approximation  $\hat{V}_{n,N}$  will get closer to  $V$  as the posterior sample size  $n$  and the auxiliary sample size  $N$  increase. Under the null hypothesis that the asymptotic distribution of the sample is equal to the target distribution, therefore, the approximate curvature diagnostic  $\hat{\mathcal{C}}_{n,N}(\mathbf{x})$  has an asymptotic  $\chi^2(r)$  distribution. A simple heuristic for determining  $N$  is to plot the approximation  $\hat{\mathbf{d}}_N(\boldsymbol{\theta})$  against the auxiliary sample size  $N$  and select  $N$  at which the approximation appears to stabilise. Similarly we choose  $n$  at which the approximation  $\hat{V}_{n,N}$  appears to stabilise for the pre-determined  $N$ . Given  $n$  and  $N$ , we reject the null hypothesis at significance level  $\alpha$  if  $\hat{\mathcal{C}}_{n,N}(\mathbf{x})$  is greater than the  $1 - \alpha$  quantile of the  $\chi^2(r)$  distribution.

The consistency of  $\hat{V}_{n,N}$  in Theorem 1 holds for i.i.d. samples. For a sample generated from a Markov process, we suggest thinning the sample such that the auto-correlation is small. In our examples we thinned samples to obtain auto-correlations below 0.1.

## 5 A kernel Stein discrepancy

In this section we briefly describe an inverse multiquadric kernel Stein discrepancy (IMQ KSD) introduced by Gorham and Mackey (2017) and develop a Monte Carlo approximate version, AIKS (approximate inverse multiquadric kernel Stein discrepancy), for use with doubly intractable target distributions. IMQ KSD is a kernel Stein discrepancy-based diagnostic that has theoretical support and is available in closed form. To make this approach available for models with intractable normalising functions, we develop its Monte Carlo approximation and show that AIKS asymptotically inherits the same convergence properties as IMQ KSD.

### 5.1 An inverse multiquadric kernel Stein discrepancy

Gorham and Mackey (2017) defined the inverse multiquadric kernel Stein discrepancy for assessing the quality of a sample and provided theoretical justification for its use in diagnosing convergence of a sequence of sample points to a target distribution. Consider

a target distribution  $P$  with probability density function  $\pi(\boldsymbol{\theta})$  under which direct integration is infeasible. Consider a weighted sample targeting  $P$ , which is defined as  $Q_n = \sum_{i=1}^n q_n(\boldsymbol{\theta}^{(i)})\delta_{\boldsymbol{\theta}^{(i)}}$  with i.i.d. sample  $\boldsymbol{\theta}^{(1)}, \dots, \boldsymbol{\theta}^{(n)}$  and probability mass function  $q_n$ . Suppose we want to evaluate  $E_P \{z(\boldsymbol{\theta})\}$ , which is intractable. The weighted sample  $Q_n$  provides an approximation  $E_{Q_n} \{z(\boldsymbol{\theta})\} = \sum_{i=1}^n z(\boldsymbol{\theta}^{(i)})q_n(\boldsymbol{\theta}^{(i)})$  of the target expectation. To assess the quality of the approximation, one may consider discrepancies quantifying the maximum expectation error over a set of test functions  $\mathcal{Z}$ :

$$d_{\mathcal{Z}}(Q_n, P) = \sup_{z \in \mathcal{Z}} |E_P \{z(\boldsymbol{\theta})\} - E_{Q_n} \{z(\boldsymbol{\theta})\}|.$$

When  $\mathcal{Z}$  is large enough the discrepancy is called an integral probability metric (IPM) (Müller, 1997) and  $d_{\mathcal{Z}}(Q_n, P) \rightarrow 0$  only if  $Q_n \Rightarrow P$  for any sequence  $Q_n$ . We use  $\Rightarrow$  to denote the weak convergence of a sequence of probability measures. However, it is not practical to use IPM for assessing a sample since  $E_P \{z(\boldsymbol{\theta})\}$  may not be computable for some  $z \in \mathcal{Z}$ .

According to Stein's method (Stein, 1972), Gorham and Mackey (2015) defined a Stein discrepancy as

$$\mathcal{S}(Q_n, \mathcal{T}_P, \mathcal{G}) = \sup_{g \in \mathcal{G}} |E_{Q_n} \{(\mathcal{T}_P g)(\boldsymbol{\theta})\}|$$

for a Langevin Stein operator  $\mathcal{T}_P$  and a Stein set  $\mathcal{G}$  that satisfy  $E_P \{(\mathcal{T}g)(\boldsymbol{\theta})\} = 0$  for all  $g \in \mathcal{G}$ . The Stein discrepancy is the maximum expectation error over the Stein set  $\mathcal{G}$  given the Stein operator  $\mathcal{T}_P$ . This avoids explicit integration under  $P$  by selecting appropriate  $\mathcal{T}_P$  and  $\mathcal{G}$  that lead the target expectation to zero. Gorham and Mackey (2017) selected kernel Stein set based on the inverse multiquadric kernel and defined the inverse multiquadric kernel Stein discrepancy  $\mathcal{S}(Q_n, \mathcal{T}_P, \mathcal{G}_{k, \|\cdot\|})$  for any norm  $\|\cdot\|$ , which admits closed-form solution.

**Definition 3 (Inverse Multiquadric Kernel Stein Discrepancy (IMQ KSD) (Gorham and Mackey 2017))** Let  $k(\mathbf{x}, \mathbf{y}) = (c^2 + \|\mathbf{x} - \mathbf{y}\|_2^2)^\beta$  for some  $c > 0$  and  $\beta \in (-1, 0)$ . For each

$j \in \{1, \dots, p\}$  construct the Stein kernel

$$k_0^j(\mathbf{x}, \mathbf{y}) = u_j(\mathbf{x})u_j(\mathbf{y})k(\mathbf{x}, \mathbf{y}) + u_j(\mathbf{x})\nabla_{y_j}k(\mathbf{x}, \mathbf{y}) + u_j(\mathbf{y})\nabla_{x_j}k(\mathbf{x}, \mathbf{y}) + \nabla_{x_j}\nabla_{y_j}k(\mathbf{x}, \mathbf{y}),$$

where  $u_j$  is the  $j$ th entry of the score function of the target density. Then IMQ KSD  $\mathcal{S}(Q_n, \mathcal{T}_P, \mathcal{G}_{k, \|\cdot\|}) = \|\mathbf{w}\|$ , where

$$w_j = \sqrt{\sum_{1 \leq k \neq l \leq n} q_n(\boldsymbol{\theta}^{(k)}) k_0^j(\boldsymbol{\theta}^{(k)}, \boldsymbol{\theta}^{(l)}) q_n(\boldsymbol{\theta}^{(l)})}.$$

Computation of  $\mathbf{w}$  is parallelisable over sample pairs  $(\boldsymbol{\theta}^{(k)}, \boldsymbol{\theta}^{(l)})$  and coordinates  $j$ . For a target distribution with constrained support  $[\ell_1, u_1] \times \dots \times [\ell_d, u_d]$ , Gorham and Mackey (2017) suggest using the following kernel that respects these constraints when computing the Stein kernel:

$$k_R(\mathbf{x}, \mathbf{y}) = k(\mathbf{x}, \mathbf{y}) \prod_{\{j: \ell_j > -\infty\}} (x_j - \ell_j)(y_j - \ell_j) \prod_{\{k: u_k < \infty\}} (x_k - u_k)(y_k - u_k).$$

Gorham and Mackey (2017) provided theoretical justification for its use for diagnosing convergence of a sequence  $Q_n$  to its target distribution  $P$ :

- (a) For a distantly dissipative target distribution  $P$ , if  $\mathcal{S}(Q_n, \mathcal{T}_P, \mathcal{G}_{k, \|\cdot\|}) \rightarrow 0$ , then  $Q_n \Rightarrow P$ .
- (b) For a target distribution  $P$  having Lipschitz score function with  $\mathbb{E}_P \{\|\mathbf{u}(\boldsymbol{\theta})\|_2^2\} < \infty$ , if the Wasserstein distance  $d_{\mathcal{W}_{\|\cdot\|_2}}(Q_n, P) \rightarrow 0$ , then  $\mathcal{S}(Q_n, \mathcal{T}_P, \mathcal{G}_{k, \|\cdot\|}) \rightarrow 0$ .

Liu et al. (2016) provided the asymptotic distribution of kernel Stein discrepancies (See Theorem 4.1 in Liu et al. (2016) for details). However, the asymptotic distribution does not have a closed form in general. To obtain a consistent estimate of the  $(1 - \alpha)$  quantile of the asymptotic distribution, Liu et al. (2016) suggested the bootstrap method introduced by Arcones and Gine (1992); Huskova and Janssen (1993): We repeatedly draw multinomial random variables  $(m_1, \dots, m_n) \sim M(n, (\frac{1}{n}, \dots, \frac{1}{n}))$ , compute bootstrap samples as

$\mathcal{S}^*(Q_n, \mathcal{T}_P, \mathcal{G}_{k, \|\cdot\|}) = \|\mathbf{v}\|$ , where

$$v_j = \sqrt{\sum_{1 \leq k \neq l \leq n} \left( \frac{m_k}{n} - \frac{1}{n} \right) k_0^j(\boldsymbol{\theta}^{(k)}, \boldsymbol{\theta}^{(l)}) \left( \frac{m_l}{n} - \frac{1}{n} \right)}, \quad j = 1, \dots, p,$$

and then calculate the empirical  $(1-\alpha)$  quantile  $\hat{\gamma}_{1-\alpha}$  of  $n\mathcal{S}^*(Q_n, \mathcal{T}_P, \mathcal{G}_{k, \|\cdot\|})$ . The consistency of  $\hat{\gamma}_{1-\alpha}$  has been established in Arcones and Gine (1992); Huskova and Janssen (1993). Let  $Q$  be the limiting distribution of  $Q_n$ . We reject the null hypothesis that  $Q = P$  if  $n\mathcal{S}(Q_n, \mathcal{T}_P, \mathcal{G}_{k, \|\cdot\|})$  is greater than  $\hat{\gamma}_{1-\alpha}$ . We henceforth take the bootstrap sample size to be  $b = 1,000$ .

## 5.2 An approximate inverse multiquadric kernel Stein discrepancy for intractable normalising function problems

When the target distribution  $P$  is doubly intractable, computation of IMQ KSD is not feasible. This is because IMQ KSD requires evaluating the score function of the target density. In this section we introduce an approximate version of IMQ KSD by replacing the score function with its Monte Carlo approximation. The approximate inverse multiquadric kernel Stein discrepancy is defined as follows.

**Definition 4 (Approximate Inverse Multiquadric Kernel Stein Discrepancy (AIKS))** *Let  $k(\mathbf{x}, \mathbf{y}) = (c^2 + \|\mathbf{x} - \mathbf{y}\|_2^2)^\beta$  for some  $c > 0$  and  $\beta \in (-1, 0)$ . For each  $j \in \{1, \dots, p\}$  define an approximate Stein kernel*

$$\hat{k}_0^j(\mathbf{x}, \mathbf{y}) = \hat{u}_j(\mathbf{x})\hat{u}_j(\mathbf{y})k(\mathbf{x}, \mathbf{y}) + \hat{u}_j(\mathbf{x})\nabla_{y_j}k(\mathbf{x}, \mathbf{y}) + \hat{u}_j(\mathbf{y})\nabla_{x_j}k(\mathbf{x}, \mathbf{y}) + \nabla_{x_j}\nabla_{y_j}k(\mathbf{x}, \mathbf{y}),$$

where  $\hat{u}_j$  is the  $j$ th entry of the approximate score function of the target density. Then AIKS  $\hat{\mathcal{S}}(Q_n, \mathcal{T}_P, \mathcal{G}_{k, \|\cdot\|}) = \|\hat{\mathbf{w}}\|$ , where

$$\hat{w}_j = \sqrt{\sum_{k,l=1}^n q_n(\boldsymbol{\theta}^{(k)})\hat{k}_0^j(\boldsymbol{\theta}^{(k)}, \boldsymbol{\theta}^{(l)})q_n(\boldsymbol{\theta}^{(l)})}.$$

For doubly intractable target density  $\pi(\boldsymbol{\theta} \mid \mathbf{x})$ , the score function can be approximated using (5) from Section 4.2. Under the assumptions of IMQ KSD on the target distribution, Theorem 2 quantifies the distance between AIKS and IMQ KSD for any  $L^p$  norm.

**Theorem 2** *For a target distribution  $P$  having a bounded score function and a sample distribution  $Q_n$  targeting  $P$ , let  $\mathcal{S}(Q_n, \mathcal{T}_P, \mathcal{G}_{k, \|\cdot\|_p})$  and  $\hat{\mathcal{S}}(Q_n, \mathcal{T}_P, \mathcal{G}_{k, \|\cdot\|_p})$  denote IMQ KSD and AIKS, respectively, for the sample distribution. Then*

$$\left| \hat{\mathcal{S}}(Q_n, \mathcal{T}_P, \mathcal{G}_{k, \|\cdot\|_p}) - \mathcal{S}(Q_n, \mathcal{T}_P, \mathcal{G}_{k, \|\cdot\|_p}) \right| \leq \{n^2 M \epsilon(N)\}^{1/p}$$

almost surely for bounded constant  $M$  and  $\epsilon(N) = \mathcal{O}(1/\sqrt{N})$  where  $N$  is the auxiliary sample size used to approximate the score function of the target density.

A proof of Theorem 2 is provided in the supplementary materials. If the theorem holds, AIKS will get closer to IMQ KSD as the auxiliary sample size  $N$  increases. This implies that AIKS asymptotically inherits the same convergence properties as IMQ KSD for any  $L^p$  norm. In this article we use the  $L^2$  norm,  $\beta = -1/2$ , and  $c = 1$ . We determine  $N$  at which the approximation  $\hat{\mathbf{u}}_N(\boldsymbol{\theta})$  stabilises. Given  $N$ , we employ the bootstrap method and obtain the empirical  $(1 - \alpha)$  quantile  $\hat{\gamma}_{1-\alpha}$  of  $n\hat{\mathcal{S}}^*(Q_n, \mathcal{T}_P, \mathcal{G}_{k, \|\cdot\|})$ . Let  $Q$  be the limiting distribution of  $Q_n$ . We reject the null hypothesis that  $Q = P$  if  $n\hat{\mathcal{S}}(Q_n, \mathcal{T}_P, \mathcal{G}_{k, \|\cdot\|})$  is greater than  $\hat{\gamma}_{1-\alpha}$ .

A notable special case of doubly intractable posterior distributions arises when a prior distribution has an intractable normalising constant that is a function of parameter of interest (cf. Rao et al., 2016; Vats et al., 2022). Suppose that we have a prior density  $p(\boldsymbol{\theta} \mid \boldsymbol{\eta}) = g(\boldsymbol{\theta} \mid \boldsymbol{\eta})/z(\boldsymbol{\eta})$ , where  $z(\boldsymbol{\eta})$  is intractable. If hyperprior  $k(\cdot)$  is assigned to  $\boldsymbol{\eta}$ , the posterior density is

$$\pi(\boldsymbol{\theta}, \boldsymbol{\eta} \mid \mathbf{x}) \propto \frac{g(\boldsymbol{\theta} \mid \boldsymbol{\eta})}{z(\boldsymbol{\eta})} k(\boldsymbol{\eta}) L(\boldsymbol{\theta} \mid \mathbf{x}),$$

which leads to a doubly intractable posterior distribution. Our diagnostics ACD and AIKS can be applied to this case if auxiliary variables can be generated exactly from the prior

distribution or generated by a Monte Carlo algorithm having  $p(\boldsymbol{\theta} \mid \boldsymbol{\eta})$  as its target distribution. Using the auxiliary variables, we can approximate intractable derivatives of the prior and obtain our diagnostic quantities.

## 6 Applications

Here we apply our methods to both asymptotically exact and asymptotically inexact algorithms in the context of three general classes of models with intractable normalising functions: (1) the Ising model, (2) a social network model, and (3) a Conway–Maxwell–Poisson regression model. Effective sample size (ESS), which is one of the most widely used MCMC diagnostics, is helpful for asymptotically exact methods since all chains converge to the target distribution. However, for asymptotically inexact methods, ESS is inadequate since an algorithm that mixes better might yield a poorer approximation to the target distribution. To illustrate the usefulness of our approaches for asymptotically inexact methods, we compare the approximate curvature diagnostic (ACD) and the approximate multiquadric kernel Stein discrepancy (AIKS) with ESS. We note that the application of our curvature diagnostic (CD) extends well beyond intractable normalising function problems. CD is, in principle, applicable in most any likelihood-based context where misspecification is of concern. We also study the computational complexity and the variability of our diagnostics. The code for our diagnostics is implemented in **R** (Ihaka and Gentleman, 1996) and **C++**, using the **Rcpp** and **RcppArmadillo** packages (Eddelbuettel and Francois, 2011). The calculation of ESS follows Kass et al. (1998) and Robert and Casella (2013). All code was run on dual 10-core Xeon E5-2680 processors on the Penn State high-performance computing cluster. The source code may be found in the following repository (<https://github.com/bokgyeong/Diagnostics>).

### 6.1 The Ising model

The Ising model (Lenz, 1920; Ising, 1925) is one of the most famous and important models from statistical physics and provides an approach for modeling binary images. For an  $r \times s$

lattice  $\mathbf{x} = \{x_{ij}\}$  with binary values  $x_{i,j} \in \{-1, 1\}$ , where  $i, j$  denotes the row and column, the Ising model with a parameter  $\theta \in (0, 1)$  has likelihood

$$L(\theta | \mathbf{x}) = \frac{1}{c(\theta)} \exp\{\theta S(\mathbf{x})\},$$

where

$$S(\mathbf{x}) = \sum_{i=1}^r \sum_{j=1}^{s-1} x_{i,j} x_{i,j+1} + \sum_{i=1}^{r-1} \sum_{j=1}^s x_{i,j} x_{i+1,j},$$

is the sum over all possible products of neighboring elements and imposes spatial dependence. A larger value for the dependence parameter  $\theta$  produces stronger interactions among neighboring observations. Calculation of the normalising function  $c(\theta)$  requires summation over all  $2^{rs}$  possible outcomes for the model, which is computationally infeasible even for lattices of moderate size. We carried out our simulation using perfect sampling (Propp and Wilson, 1996) on a  $30 \times 30$  lattice with the parameter setting  $\theta = 0.2$ , which represents moderate dependence.

For this example we consider three algorithms: (1) Atchadé et al. (2013)'s adaptive MCMC (ALR) algorithm, (2) Liang et al. (2016)'s adaptive exchange (AEX) algorithm, which is asymptotically exact, which is asymptotically exact, and (3) Liang (2010)'s double Metropolis–Hastings (DMH) algorithm, which is asymptotically inexact. The ALR algorithm introduces multiple particles  $\boldsymbol{\theta}^{(1)}, \dots, \boldsymbol{\theta}^{(d)}$  over the parameter space and approximates  $c(\boldsymbol{\theta})$  in the Metropolis–Hastings acceptance probability using a linear combination of importance sampling estimates for  $c(\boldsymbol{\theta})/c(\boldsymbol{\theta}^{(1)}), \dots, c(\boldsymbol{\theta})/c(\boldsymbol{\theta}^{(d)})$ . The AEX algorithm runs two chains simultaneously: an auxiliary chain and a target chain. The auxiliary chain simulates a sample from a set of distributions,  $\{h(\mathbf{x} | \boldsymbol{\theta}^{(1)})/c(\boldsymbol{\theta}^{(1)}), \dots, h(\mathbf{x} | \boldsymbol{\theta}^{(d)})/c(\boldsymbol{\theta}^{(d)})\}$ , where  $\boldsymbol{\theta}^{(1)}, \dots, \boldsymbol{\theta}^{(d)}$  are predetermined particles over the parameter space, and stores the generated sample at each iteration. The target chain generates a posterior sample via the exchange algorithm (Murray et al., 2006), where an auxiliary variable  $\mathbf{y}$  is sampled from the cumulative samples in the auxiliary chain instead of exact sampling of  $\mathbf{y}$ . The DMH algorithm is asymptotically inexact but was found to be very efficient in terms of effective sample size per unit time and is applicable for doubly intractable problems with higher pa-

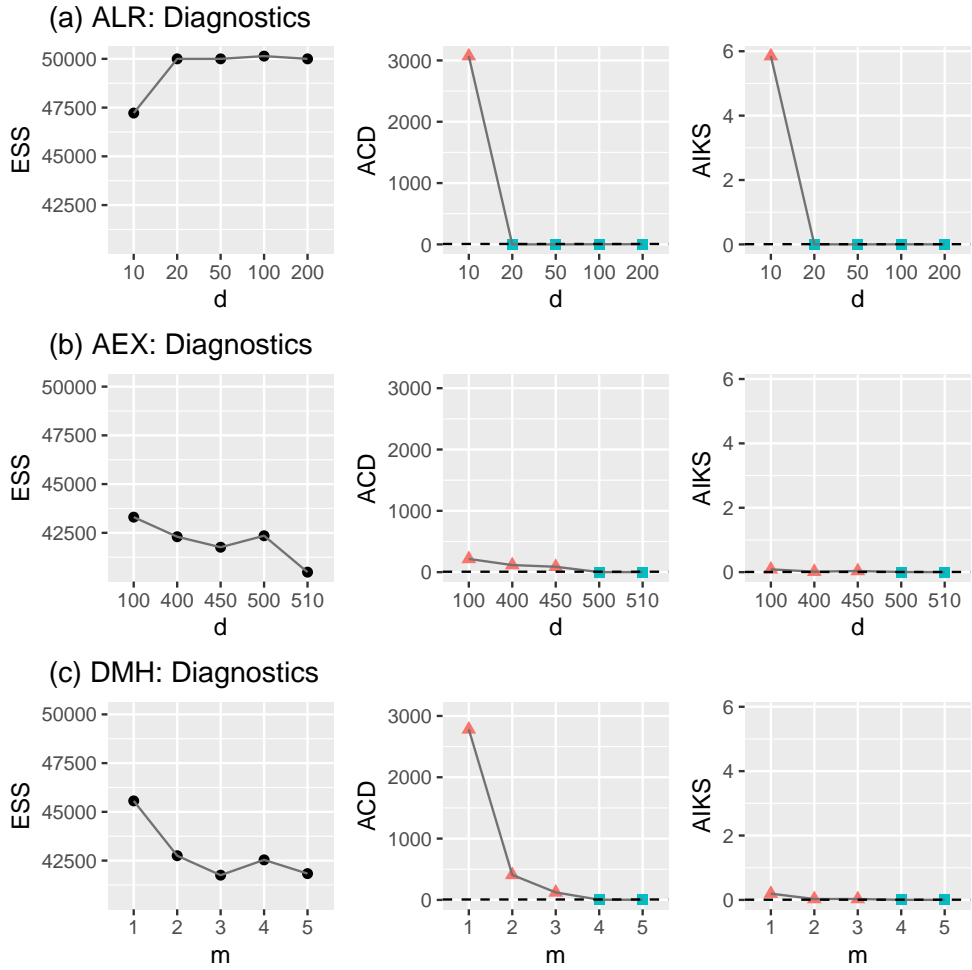


Figure 1: Results for a simulated binary lattice from the Ising model with  $\theta = 0.2$ . **(a)** Diagnostics (ESS, ACD, and AIKS) applied to samples generated from ALR with different numbers  $d$  of particles. **(b)** Diagnostics applied to samples generated from AEX with different numbers  $d$  of particles. **(c)** Diagnostics applied to samples generated from DMH with different numbers  $m$  of (inner) Gibbs updates. A larger ESS is better. For ACD and AIKS, the dashed horizontal lines represent their critical values, and the red triangles and blue squares indicate poor sample quality and good sample quality, respectively, from the hypothesis tests. For ALR, all of the diagnostics recommend  $d$  of 20 or more. For AEX, ESS recommends  $d = 100$ , while ACD and AIKS recommend  $d$  of at least 500. For DMH, ESS recommends  $m = 1$ , while ACD and AIKS recommend  $m$  of 4 or more.

parameter dimension. DMH replaces the exact sampling of  $\mathbf{y}$  in the exchange algorithm with a standard Metropolis–Hastings algorithm, an “inner sampler,” at each iteration. To find appropriate values for the tuning parameters of the algorithms, we generate multiple chains from each algorithm with different choices of tuning parameters. We implement AEX with

different numbers  $d$  of particles, where particles are selected from fractional DMH, which is DMH with a larger acceptance probability. The choice of the other tuning parameters follows Park and Haran (2018). We implement ALR with different numbers  $d$  of particles, where the particles are chosen from a short run of DMH with a single cycle of (inner) Gibbs updates. The choice of other components to be tuned follows Park and Haran (2018). We implement DMH with different numbers  $m$  of (inner) Gibbs updates. We use a uniform prior with range  $[0, 1]$  for  $\theta$ .

All algorithms were run for 1,000,000 iterations. To reduce auto-correlation in order to make the samples approximately independent, thereby satisfying conditions for theorem 1, we thinned the samples at equally spaced intervals of 20 to obtain auto-correlation below 0.1 and the length  $n = 50,000$  of samples. For ACD and AIKS,  $N = 200,000$  auxiliary variables were generated via Gibbs sampling for approximating  $\mathbf{d}(\boldsymbol{\theta})$  for ACD and  $\mathbf{u}(\boldsymbol{\theta})$  for AIKS at each posterior sample point. The posterior sample size  $n$  and the auxiliary sample size  $N$  were determined by the heuristics stated in Sections 4.2 and 5.2 (see supplement for details). We used parallel computing to obtain the approximations and to compute AIKS. For a posterior sample path, the approximation step took about 10.48 hours. The critical value of ACD is the 0.99 quantile of  $\chi^2(1)$ , which is 6.63. For AIKS we estimate the 0.99 quantile of its asymptotic distribution via the bootstrap method for a single sample path and use this critical value for assessing all samples. Given the approximations, the bootstrap procedure took approximately 10.67 hours and provided 0.006 for the critical value of AIKS. ACD computation took approximately 0.0026 seconds and AIKS computation took approximately 25.13 seconds, given the approximations.

Figure 1 (a) shows the diagnostic values for ALR for various values of  $d$ . All diagnostics provide the same conclusion that ALR requires  $d$  of 20 or more. For AEX and DMH, ACD and AIKS provide considerably different conclusions from ESS. In Figure 1 (b) it is observed that ESS is maximised (the best) at  $d = 100$  and generally decreases (worsens) as  $d$  increases for AEX. On the other hand, both ACD and AIKS have their largest (worst) values at  $d = 100$  and indicate that  $d$  should be at least 500. Likewise, for DMH, Figure 1 (c) shows that ESS is maximised (the best) at  $m = 1$  and generally decreases (worsens) as

Table 1: Summary statistics and walltimes of ESS-, ACD-, and AIKS-selected samples for each algorithm and a gold standard in the Ising model for a simulated binary lattice.

	Algorithm	$d$ or $m$	Median	SD	LTP	RTP	LCP	RCP	Time (hr)
ESS-selected	ALR	100	0.19	0.02	0.05	0.05	0.05	0.05	20.78
	AEX	100	0.19	0.02	0.05	0.05	0.05	0.06	12.95
	DMH	1	0.19	0.03	0.09	0.04	0.04	0.09	0.03
ACD & AIKS -selected	ALR	20	0.19	0.02	0.05	0.05	0.05	0.05	20.78
	AEX	500	0.19	0.02	0.05	0.05	0.05	0.05	55.29
	DMH	4	0.19	0.02	0.05	0.05	0.05	0.05	0.11
Gold standard			0.19	0.02	0.05	0.05	0.05	0.05	

SD, standard deviation; LTP, left-tail probability; RTP, right-tail probability; LCP, left-center probability; RCP, right-center probability.

$m$  increases, while ACD and AIKS take their largest (worst) values at  $m = 1$  and decrease (improve) as  $m$  increases, both recommending  $m$  of 4 or more.

Table 1 presents summary statistics of ESS-, ACD-, and AIKS-selected samples for each algorithm. The ESS-selected sample has the tuning parameter value that provides the largest ESS. The ACD-, and AIKS-selected samples are their hypothesis test-based good-quality samples with the smallest possible tuning parameter value. ESS selects ALR with  $d = 100$ , AEX with  $d = 100$ , and DMH with  $m = 1$ . Both ACD and AIKS choose ALR with  $d = 20$ , AEX with  $d = 500$ , and DMH with  $m = 4$ . We use the sample generated from the exchange algorithm (Murray et al., 2006), which is asymptotically exact and has no tuning parameter, as the gold standard. Cutoff values for the left- and right-tail probabilities are the lower 5% and the upper 5% percentiles of the gold standard. Cutoff values for the left-center probability are the lower 45% percentile and median of the gold standard. Cutoff values for the right-center probability are the median and upper 45% percentile of the gold standard. It is observed that the ACD- and AIKS-selected samples provide the same values of the summary statistics as the gold standard. ACD and AIKS imply that DMH with  $m = 4$  is computationally much more efficient than the other algorithms and provides good-quality samples. On the other hand, the ESS-selected AEX and DMH samples do not match the gold standard. The ESS-selected AEX sample has a slightly higher right-center probability. The ESS-selected DMH sample provides a larger standard deviation, higher tail probabilities, and lower center probabilities. This shows that ACD and AIKS

perform well in assessing how close samples are to the exact posterior. Not surprisingly, ESS is inadequate as a tool for this purpose. In summary, our approaches provide good guidance on how to assess the quality of samples for both the asymptotically exact and asymptotically inexact algorithms. In addition, our diagnostics help one to select the best algorithm and its tuning parameter in terms of computational efficiency.

## 6.2 A social network model

An exponential family random graph model (ERGM) (Robins et al., 2007; Hunter et al., 2008) is a statistical model for analysing network data. Consider an undirected ERGM with  $n$  vertices. Relationships among the vertices can be represented as an  $n \times n$  adjacency matrix  $\mathbf{x}$  as follows: for all  $i \neq j$ ,  $x_{i,j} = 1$  if the  $i$ th and  $j$ th vertices are connected, and  $x_{i,j} = 0$  otherwise. And  $x_{i,i}$  is 0 for all  $i \in \{1, \dots, n\}$ , i.e., there are no loops. The number of possible network configurations is  $2^{n(n-1)/2}$  and summation over those configurations is required to calculate the normalising function of the model. Thus computing  $c(\boldsymbol{\theta})$  is infeasible unless  $n$  is quite small.

For an undirected graph with  $n$  vertices, the ERGM likelihood is given by

$$\begin{aligned} L(\boldsymbol{\theta} | \mathbf{x}) &= \frac{1}{c(\boldsymbol{\theta})} \exp\{\theta_1 S_1(\mathbf{x}) + \theta_2 S_2(\mathbf{x})\}, \\ S_1(\mathbf{x}) &= \sum_{i=1}^n \begin{pmatrix} x_{i+} \\ 1 \end{pmatrix}, \\ S_2(\mathbf{x}) &= e^\tau \sum_{k=1}^{n-2} \{1 - (1 - e^{-\tau})^k\} \text{EP}_k(\mathbf{x}). \end{aligned}$$

The sufficient statistics  $S_1(\mathbf{x})$  and  $S_2(\mathbf{x})$  are the number of edges in the graph and the geometrically weighted edge-wise shared partnership (GWESP) statistic (Hunter and Handcock, 2006; Hunter, 2007), respectively.  $x_{i+}$  denotes the sum of the  $i$ th row of the adjacency matrix and  $\text{EP}_k(\mathbf{x})$  denotes the number of edges between two vertices that share exactly  $k$  neighbors. It is assumed that  $\tau$  is fixed at a value of 0.25. We simulated a network with 30 actors using 10,000 cycles of Gibbs updates, where the true parameter was

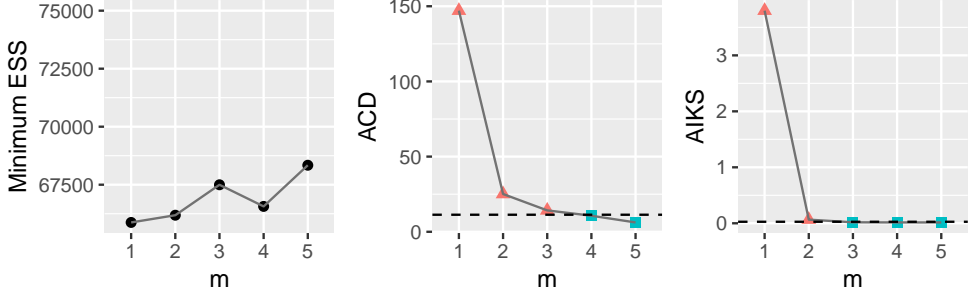


Figure 2: Results for a simulated network from ERGM with  $\boldsymbol{\theta} = (\theta_1, \theta_2)^\top = (-0.96, 0.04)^\top$ . Diagnostics (minimum ESS, ACD, and AIKS) applied to samples generated from DMH with different numbers  $m$  of (inner) Gibbs updates. A larger ESS is better. For ACD and AIKS, the dashed horizontal lines represent their critical values, and the red triangles and blue squares indicate poor sample quality and good sample quality, respectively, from the hypothesis tests. The minimum ESS recommends  $m = 5$  and does not recommend  $m = 20$ . ACD recommends  $m$  of at least 4 and AIKS recommends  $m$  of 3 or more.

$$\boldsymbol{\theta} = (\theta_1, \theta_2)^\top = (-0.96, 0.04)^\top.$$

For this example we consider the DMH algorithm, which is asymptotically inexact. We explained the DMH algorithm in Section 6.1. We implement DMH with different numbers  $m$  of Gibbs updates. We use uniform priors with range  $[-5.00, 2.27] \times [-1.57, 2.32]$  for  $(\theta_1, \theta_2)^\top$ , which are centered around the maximum pseudo-likelihood estimates (MPLE) and have widths of 12 standard deviations.

The algorithm was run for 1,875,000 iterations. To reduce auto-correlation in order to make the samples approximately independent, thereby satisfying conditions for theorem 1, we thinned the samples at equally spaced intervals of 25 to obtain auto-correlation below 0.1 and the length  $n = 75,000$  of sample points. For ACD and AIKS,  $N = 200,000$  auxiliary variables were generated via Gibbs sampling for approximating  $\mathbf{d}(\boldsymbol{\theta})$  for ACD and  $\mathbf{u}(\boldsymbol{\theta})$  for AIKS at each posterior sample point. The posterior sample size  $n$  and the auxiliary sample size  $N$  were chosen as in the previous example (see supplement for details). We used parallel computing to obtain the approximations and to compute AIKS. For a posterior sample path, the approximation step took approximately 43.79 hours. The critical value of ACD is the 0.99 quantile of  $\chi^2(3)$ , which is 11.34. For AIKS we estimate the 0.99 quantile of its asymptotic distribution via the bootstrap method for a single sample path and use this critical value for assessing all samples. Given the approximations, the bootstrap

Table 2: Summary statistics and walltimes of ESS-, ACD-, and AIKS-selected DMH samples and a gold standard for  $\theta_1$  in ERGM for a simulated network.

	Algorithm	$m$	Median	SD	LTP	RTP	LCP	RCP	Time (hr)
ESS-selected	DMH	5	-1.13	0.53	0.05	0.05	0.05	0.05	2.97
ACD-selected	DMH	4	-1.13	0.53	0.05	0.05	0.05	0.05	1.85
AIKS-selected	DMH	3	-1.13	0.53	0.05	0.05	0.05	0.05	1.66
Gold standard			-1.13	0.53	0.05	0.05	0.05	0.05	

SD, standard deviation; LTP, left-tail probability; RTP, right-tail probability; LCP, left-center probability; RCP, right-center probability.

procedure took approximately 20.31 hours and provided 0.027 for the critical value of AIKS. ACD computation took approximately 0.0066 seconds and AIKS computation took approximately 2 minutes, given the approximations.

Figure 2 shows minimum effective sample size, ACD, and AIKS for the DMH sample for a sequence of  $m$  values. The minimum ESS generally increases (becomes better) as  $m$  increases and is maximised (the best) at  $m = 5$ . ACD and AIKS also generally decrease (become better) as  $m$  increases. ACD implies that  $m$  should be at least 4, and AIKS suggests that  $m$  should be at least 3.

Table 2 presents summary statistics of ESS-, ACD-, and AIKS-selected DMH samples. The ESS-selected sample has the tuning parameter value that provides the largest ESS. The ACD-, and AIKS-selected samples are their hypothesis test-based good-quality samples with the smallest possible tuning parameter value. ESS selects  $m = 5$ , ACD chooses  $m = 4$ , and AIKS selects  $m = 3$ . We treat a run from DMH with 20 cycles of Gibbs updates as the gold standard. Both ACD and AIKS indicate good sample quality (ACD = 0.66 and AIKS = 0.016). The cutoff values for left- and right-tail probabilities and left- and right-center probabilities are chosen as in the previous example (see supplement for details). We observe that all ESS-, ACD-, and AIKS-selected samples provide the same values of the summary statistics as the gold standard. In this case, all the diagnostics generally agree.

### 6.3 A Conway–Maxwell–Poisson regression model

The Conway–Maxwell–Poisson (COMP) distribution (Conway and Maxwell, 1962) is a two-parameter generalisation of the Poisson distribution for modeling count data that are char-

acterised by under-dispersion (variance less than the mean) or over-dispersion (variance greater than the mean). For a  $\text{COMP}(\lambda, \nu)$  variable  $Y$ , the probability mass function is given by

$$P(Y = y) = \frac{1}{c(\lambda, \nu)} \frac{\lambda^y}{(y!)^\nu},$$

where  $\lambda > 0$  is a generalisation of the Poisson rate parameter,  $\nu \geq 0$  denotes the dispersion parameter, and  $c(\lambda, \nu) = \sum_{z=0}^{\infty} \frac{\lambda^z}{(z!)^\nu}$  is a normalising function. The COMP distribution accommodates under- ( $\nu > 1$ ), equi- ( $\nu = 1$ ), or over-dispersion ( $0 \leq \nu < 1$ ). The COMP distribution forms a continuous bridge between the Poisson ( $\nu = 1$ ), geometric ( $\nu = 0$  and  $\lambda < 1$ ), and Bernoulli ( $\nu = \infty$  and success probability  $\lambda/(1 + \lambda)$ ) distributions. Guikema and Goffelt (2008) proposed a reparameterisation, substituting  $\eta = \lambda^{1/\nu}$  to approximate the center of the COMP distribution. For a count variable  $Y$  that follows the  $\text{COMP}_\eta(\eta, \nu)$  distribution, the probability mass function is

$$P(Y = y) = \frac{1}{c_\eta(\eta, \nu)} \left( \frac{\eta^y}{y!} \right)^\nu,$$

where  $c_\eta(\eta, \nu) = \sum_{z=0}^{\infty} \left( \frac{\eta^z}{z!} \right)^\nu$  is the normalising function. Huang (2017) and Ribeiro et al. (2020) have reparameterised the COMP distribution as a function of the mean. Under any parameterisation, however, the COMP normalising function is an infinite sum, making the function intractable.

For count response variables  $Y_i$  and corresponding explanatory variables  $\mathbf{x}_i = (x_{i,1}, \dots, x_{i,p-1})^\top$  for  $i = 1, \dots, n$ , the likelihood of a COMP regression model with log link function for  $\eta$  is given by

$$Y_i \sim \text{COMP}_\eta(\eta_i, \nu),$$

$$\log(\eta_i) = \beta_0 + x_{i,1}\beta_1 + \dots + x_{i,p-1}\beta_{p-1}, \quad i = 1, \dots, n,$$

where  $\boldsymbol{\beta} = (\beta_0, \dots, \beta_{p-1})^\top$  are regression coefficients. We study the takeover bids dataset (Cameron and Johansson, 1997), which comprises the number of bids received by 126 US

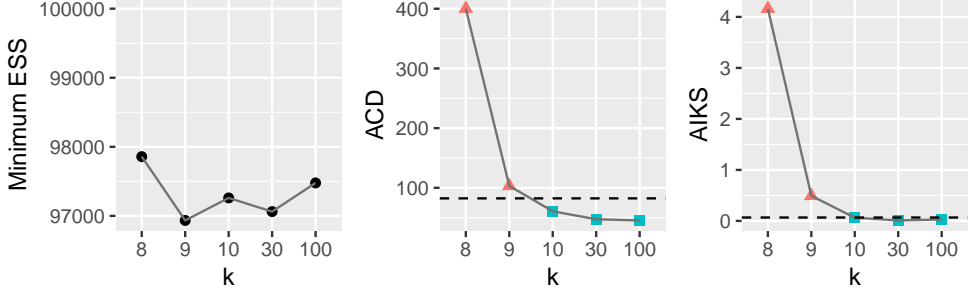


Figure 3: Results for the takeover bids dataset in the COMP regression model. Diagnostics (minimum ESS, ACD, and AIKS) applied to samples generated from NormTrunc with different levels  $k$  of truncation. A larger ESS is better. For ACD and AIKS, the dashed horizontal lines represent their critical values, and the red triangle and blue square imply poor sample quality and good sample quality, respectively, from the hypothesis tests. The minimum ESS recommends  $k = 8$ . ACD and AIKS recommend  $k$  of 10 or more.

firms that were targets of tender offers during the period 1978–1985, along with 9 explanatory variables (see Sáez-Castillo and Conde-Sánchez, 2013, for details). The dataset can be obtained from `mpcnp` package (Fung et al., 2019). It is assumed that  $\nu$  is fixed at a value of 1.754 (Huang, 2017).

For this example we consider a simple and widely used approach, namely, the NormTrunc algorithm. Specifically, we approximate the normalising function by truncating the infinite sum to a truncation level  $k$  such that  $c_\eta(\eta, \nu) \approx \sum_{z=0}^k \left(\frac{\eta^z}{z!}\right)^\nu$  and use the approximation for each Metropolis–Hastings accept-reject ratio. The NormTrunc algorithm is asymptotically inexact. In order to determine a suitable value of  $k$ , we implement NormTrunc with different levels  $k$  of truncation.

The algorithm was run for 10,000,000 iterations. To reduce auto-correlation in order to make the samples approximately independent, thereby satisfying conditions for theorem 1, we thinned the samples at equally spaced intervals of 100 to obtain auto-correlation below 0.1 and the length  $n = 100,000$  of sample points. For ACD and AIKS,  $N = 200,000$  auxiliary variables were generated via Chanialidis et al. (2018)’s rejection sampling algorithm for approximating  $\mathbf{d}(\boldsymbol{\theta})$  for ACD and  $\mathbf{u}(\boldsymbol{\theta})$  for AIKS at each posterior sample point. The posterior sample size  $n$  and the auxiliary sample size  $N$  were determined as in the previous example (see supplement for details). We used parallel computing to obtain the approximations and to compute AIKS. For a posterior sample path, the approximation step

Table 3: Summary statistics and walltimes of ESS-, ACD-, and AIKS-selected NormTrunc samples and a gold standard for  $\beta_7$  in the COMP regression model for the takeover bids dataset.

	Algorithm	$k$	Median	SD	LTP	RTP	LCP	RCP	Time (min)
ESS-selected	NormTrunc	8	0.50	0.14	0.05	0.05	0.05	0.06	25.19
ACD & AIKS-selected	NormTrunc	10	0.49	0.13	0.05	0.05	0.05	0.05	39.72
Gold standard			0.49	0.13	0.05	0.05	0.05	0.05	

SD, standard deviation; LTP, left-tail probability; RTP, right-tail probability; LCP, left-center probability; RCP, right-center probability.

took approximately 7.96 hours. The critical value of ACD is the 0.99 quantile of  $\chi^2(55)$ , which is 82.29. For AIKS we estimate the 0.99 quantile of its asymptotic distribution via the bootstrap method for a single sample path and use this critical value for assessing all samples. Given the approximations, the bootstrap procedure took approximately 197.37 hours and provided 0.102 for the critical value of AIKS. ACD computation took approximately 0.3421 seconds and AIKS computation took approximately 19.25 minutes, given the approximations.

Figure 3 shows minimum effective sample size, ACD, and AIKS for the NormTrunc sample for an array of  $k$  values. ACD and AIKS provide considerably different conclusions from ESS. The minimum ESS is maximised (the best) at  $k = 8$ . On the other hand, both ACD and AIKS take their largest (worst) values at  $k = 8$  and decrease (improve) as  $k$  increases. Both recommend  $k$  of 10 or more.

Table 3 presents summary statistics of ESS-, ACD-, and AIKS-selected NormTrunc samples. The ESS-selected sample has the tuning parameter value that provides the largest ESS. The ACD- and AIKS-selected samples are their hypothesis test-based good-quality samples with the smallest possible tuning parameter value. ESS selects  $k = 8$ , and both ACD and AIKS choose  $k = 100$ . We treat as the gold standard a run from the exchange algorithm (Murray et al., 2006), where auxiliary variables are generated from the data model with  $\hat{c}_\eta(\eta, \nu) = \sum_{z=0}^{100} \left(\frac{\eta^z}{z!}\right)^\nu$  as its normalising function. Both ACD and AIKS indicate good sample quality (ACD = 63.98 and AIKS = 0.061). The cutoff values for left- and right-tail probabilities and left- and right-center probabilities were chosen as in the previous example. It is found that the ACD- and AIKS-selected sample provide the same values of the

summary statistics as the gold standard. On the other hand, the ESS-selected sample has a slightly large median, large standard deviation, and high right-center probability compared to the gold standard. In summary, our approaches help tune algorithms. In particular, for asymptotically inexact algorithms, our methods can guide users to appropriately choose their tuning parameters and help provide reliable inference.

## 6.4 Computational complexity

We examine the computational complexity of the approximate curvature diagnostic (ACD) and the approximate inverse multiquadric kernel Stein discrepancy (AIKS), summarising how our diagnostics scale with an increase in the size  $n$  of posterior samples and the size  $N$  of auxiliary samples.

We denote by  $s$  the computational cost of simulating a single auxiliary variable and calculating the derivatives given the auxiliary variable for approximating the intractable terms discussed in Section 4.2. Using  $N$  auxiliary variables, we approximate  $\mathbf{d}(\boldsymbol{\theta})$  for ACD and  $\mathbf{u}(\boldsymbol{\theta})$  for AIKS at each posterior sample point. The complexity of the approximation step is  $\mathcal{O}(nsN)$ . Given the approximations, the complexity for estimating the critical value of AIKS is  $\mathcal{O}(bn^2)$ , where  $b$  is the bootstrap sample size. The complexity for ACD is  $\mathcal{O}(n)$  and the complexity for AIKS is  $\mathcal{O}(n^2)$ , given the approximations. It is important

Table 4: Summary statistics for 100 replicates and critical values of ACD and AIKS in the COMP regression model for the takeover bids dataset.

Diagnostic	$k$	Mean	SD	Min	Max	Critical value
ACD	8	399.99	0.13	399.61	400.36	82.29
	9	103.09	0.07	102.94	103.28	
	10	60.57	0.06	60.44	60.69	
	30	47.29	0.05	47.18	47.41	
	100	45.23	0.06	45.09	45.37	
AIKS	8	4.162	0.00093	4.1603	4.1652	0.102
	9	0.492	0.00029	0.4915	0.4928	
	10	0.063	0.00009	0.0628	0.0632	
	30	0.009	0.00002	0.0092	0.0093	
	100	0.028	0.00006	0.0279	0.0282	

SD, standard deviation.

to note that the approximation step and computation of AIKS and its critical value are embarrassingly parallelisable.

## 6.5 Variability of diagnostics

In this section we investigate the variability of ACD and AIKS using the example in Section 6.3. We create 100 replicates of our diagnostics for each posterior sample path. Table 4 shows summary statistics for the replicates. We see that ACD and AIKS have very small standard deviations. Both ACD and AIKS recommend  $k$  of at least 10 based on their maximum values, which shows that they provide the same conclusion across 100 replicates. This implies that the variability of our diagnostic quantities can be controlled by selecting suitable values of tuning parameters; auxiliary sample size  $N$  and posterior sample size  $n$  for ACD; and auxiliary sample size  $N$  for AIKS.

## 7 Discussion

In this article we proposed new methods that provide guidance for tuning algorithms and give some measure of sample quality for a wide range of Monte Carlo algorithms, including a particularly challenging class of algorithms: asymptotically inexact algorithms for distributions with intractable normalising functions. We describe three methods. CD applies broadly to most any likelihood-based context where misspecification is of concern while ACD and AIKS are specifically targeted at likelihoods with intractable normalising functions. Our study mainly focuses on intractable normalising function problems and shows that our methods can assess the quality of samples and provide good guidance for tuning algorithms. We have studied applications of ACD and AIKS to several asymptotically exact and inexact algorithms in the context of challenging simulated and real data examples. This shows that our methods provide useful results not only for asymptotically exact algorithms, for which some other methods may be useful, but also for asymptotically inexact algorithms, for which we are not aware of other methods.

There are of course simple and reasonable heuristics one can use for diagnostic pur-

poses, such as increasing  $m$  until DMH approximations stabilise. However, our diagnostics go beyond simple approaches, allowing one to compare sample quality across different algorithms, including comparing asymptotically exact algorithms with asymptotically inexact algorithms.

We note that ACD and AIKS could be slightly different in their conclusions as the example in Section 6.2 illustrates, but the difference is quite small and overall conclusions are pretty much the same. The difference between ACD and AIKS stems from the fact that they consider different sets of test functions to quantify the difference between a sample mean and a target expectation. ACD considers two functions whose target expectations are identical and measures the difference between sample means of the two functions. AIKS considers a set of functions whose target expectations are zero and finds the maximum error between the sample mean and the target expectation. Unless the score function of the target density is the origin, their sets of test functions are mutually exclusive, which is the case of all the examples in this article. Depending on the setting, one of ACD or AIKS may be more useful than the other. ACD has a  $\chi^2$  distribution as its asymptotic distribution, which permits a fixed critical value to be used for testing the null hypothesis. AIKS, on the other hand, requires a bootstrap procedure for estimating its critical value, which can be computationally expensive for a large sample size  $n$  or high parameter dimension  $p$ ; this is the case for the example discussed in Section 6.3. However, one advantage of AIKS is that it is supported by a theory of weak convergence and thus can be used for deciding convergence of a sequence of sample points to the target distribution.

ACD and AIKS are obtained by replacing some functions that have to be evaluated for CD and IMQ KSD with their Monte Carlo approximations. This allows for the diagnostics to be available for doubly intractable posterior distributions. The computing time of ACD and AIKS mainly accounts for the Monte Carlo approximation, which might be computationally expensive for high-dimensional datasets. However, the approximation step is embarrassingly parallel in that the Monte Carlo estimates at the posterior sample points can be constructed entirely in parallel. Therefore, the computational expense can be decreased by a factor corresponding to the number of available cores. This can be help-

ful provided that the availability of parallel computing resources increases. An important caveat of ACD is that it can be misled if the first two moments match the target distribution but higher order moments do not. AIKS cannot be misled in such fashion. Developing fast approaches for obtaining the approximations and extending ACD to higher order moments may provide interesting avenues for future research.

## Acknowledgements

The authors are grateful to Jaewoo Park for providing useful code and to Galin Jones and Geoff K. Nicholls for illuminating discussions. JH and MH were partially supported by the National Institute of General Medical Sciences of the National Institutes of Health under Award Number R01GM123007.

## References

Alquier, P., Friel, N., Everitt, R., and Boland, A. (2016). Noisy Monte Carlo: Convergence of Markov chains with approximate transition kernels. *Statistics and Computing*, 26(1-2):29–47.

Andrieu, C. and Roberts, G. O. (2009). The pseudo-marginal approach for efficient Monte Carlo computations. *Annals of Statistics*, 37:697–725.

Arcones, M. A. and Gine, E. (1992). On the bootstrap of U and V statistics. *The Annals of Statistics*, 20:655–674.

Atchadé, Y. F., Lartillot, N., and Robert, C. (2013). Bayesian computation for statistical models with intractable normalizing constants. *Brazilian Journal of Probability and Statistics*, 27(4):416–436.

Bartlett, M. S. (1953a). Approximate confidence intervals. *Biometrika*, 40(1/2):12–19.

Bartlett, M. S. (1953b). Approximate confidence intervals. II. More than one unknown parameter. *Biometrika*, 40(3/4):306–317.

Beaumont, M. A. (2003). Estimation of population growth or decline in genetically monitored populations. *Genetics*, 164.

Besag, J. (1974). Spatial interaction and the statistical analysis of lattice systems. *Journal of the Royal Statistical Society: Series B*, 36(2):192–225.

Cameron, A. C. and Johansson, P. (1997). Count data regression using series expansions: With applications. *Journal of Applied Econometrics*, 12:203–223.

Chanialidis, C., Evers, L., Neocleous, T., and Nobile, A. (2018). Efficient Bayesian inference for COM-Poisson regression models. *Statistics and Computing*, 28:595–608.

Chazottes, J. R., Collet, P., Külske, C., and Redig, F. (2007). Concentration inequalities for random fields via coupling. *Probability Theory and Related Fields*, 137:201–225.

Cheng, J., Li, T., Levina, E., and Zhu, J. (2017). High-dimensional mixed graphical models. *Journal of Computational and Graphical Statistics*, 26:367–378.

Conway, R. W. and Maxwell, W. L. (1962). Network dispatching by the shortest-operation discipline. *Operations Research*, 10:51–73.

Cowles, M. K. and Carlin, B. P. (1996). Markov chain Monte Carlo convergence diagnostics: A comparative review. *Journal of the American Statistical Association*, 91(434):883–904.

Damerdji, H. (1994). Strong consistency of the variance estimator in steady-state simulation output analysis. *Mathematics of Operations Research*, 19:494–512.

Eddelbuettel, D. and Francois, R. (2011). Rcpp: Seamless R and C++ integration. *Journal of Statistical Software*, 40:1–18.

Fan, Y., Brooks, S. P., and Gelman, A. (2006). Output assessment for Monte Carlo simulations via the score statistic. *Journal of Computational and Graphical Statistics*, 15(1):178–206.

Flegal, J. M., Haran, M., and Jones, G. L. (2008). Markov chain monte carlo: Can we trust the third significant figure? *Statistical Science*, pages 250–260.

Flegal, J. M. and Jones, G. L. (2011). Implementing MCMC: Estimating with confidence. In *Handbook of Markov Chain Monte Carlo*, chapter 7, pages 175–197. CRC Press.

Fung, H.-T., Alwan, A., Wishart, J., and Huang, A. (2019). mpcmp: Mean-parametrized conway-maxwell poisson regression.

Goldstein, J., Haran, M., Simeonov, I., Fricks, J., and Chiaromonte, F. (2015). An attraction-repulsion point process model for respiratory syncytial virus infections. *Biometrics*, 71(2):376–385.

Gorham, J. and Mackey, L. (2015). Measuring sample quality with Stein’s method. In *Advances in Neural Information Processing Systems*, volume 28, pages 226–234.

Gorham, J. and Mackey, L. (2017). Measuring sample quality with kernels. In *Proceedings of the 34th International Conference on Machine Learning*, volume 70 of *Proceedings of Machine Learning Research*, pages 1292–1301.

Guikema, S. D. and Goffelt, J. P. (2008). A flexible count data regression model for risk analysis. *Risk Analysis*, 28:213–223.

Hastings, W. K. (1970). Monte Carlo sampling methods using Markov chains and their applications. *Biometrika*, 57(1):97–109.

Huang, A. (2017). Mean-parametrized Conway–Maxwell–Poisson regression models for dispersed counts. *Statistical Modelling*, 17:359–380.

Hughes, J., Haran, M., and Caragea, P. C. (2011). Autologistic models for binary data on a lattice. *Environmetrics*, 22(7):857–871.

Hunter, D. R. (2007). Curved exponential family models for social networks. *Social Networks*, 29(2):216–230.

Hunter, D. R. and Handcock, M. S. (2006). Inference in curved exponential family models for networks. *Journal of Computational and Graphical Statistics*, 15(3):565–583.

Hunter, D. R., Handcock, M. S., Butts, C. T., Goodreau, S. M., and Morris, M. (2008). ergm: A package to fit, simulate and diagnose exponential-family models for networks. *Journal of Statistical Software*, 24(3):1–29.

Huskova, M. and Janssen, P. (1993). Consistency of the generalized bootstrap for degenerate U-statistics. *The Annals of Statistics*, 21:1811–1823.

Ihaka, R. and Gentleman, R. (1996). R: A language for data analysis and graphics. *Journal of Computational and Graphical Statistics*, 5(3):299–314.

Ising, E. (1925). Beitrag zur theorie des ferromagnetismus. *Zeitschrift für Physik A Hadrons and Nuclei*, 31(1):253–258.

Jones, G. L., Haran, M., Caffo, B. S., and Neath, R. (2006). Fixed-width output analysis for Markov chain Monte Carlo. *Journal of the American Statistical Association*, 101:1537–1547.

Kass, R. E., Carlin, B. P., Gelman, A., and Neal, R. M. (1998). Markov Chain Monte Carlo in Practice: A Roundtable Discussion. *The American Statistician*, 52(2):93–100.

Lauritzen, S. L. and Wermuth, N. (1989). Graphical models for associations between variables, some of which are qualitative and some quantitative. *The Annals of Statistics*, 17:31–57.

Lee, J. D. and Hastie, T. J. (2015). Learning the structure of mixed graphical models. *Journal of Computational and Graphical Statistics*, 24:230–253.

Lee, J. E., Nicholls, G. K., and Ryder, R. J. (2019). Calibration Procedures for Approximate Bayesian Credible Sets. *Bayesian Analysis*, 14(4):1245–1269.

Lenz, W. (1920). Beitrag zum Verständnis der magnetischen Erscheinungen in festen Körpern. *Physikalische Zeitschrift*, 21:613–615.

Liang, F. (2010). A double Metropolis-Hastings sampler for spatial models with intractable normalizing constants. *Journal of Statistical Computation and Simulation*, 80(9):1007–1022.

Liang, F., Jin, I. H., Song, Q., and Liu, J. S. (2016). An adaptive exchange algorithm for sampling from distributions with intractable normalizing constants. *Journal of the American Statistical Association*, 111(513):377–393.

Liu, Q., Lee, J. D., and Jordan, M. (2016). A kernelized Stein discrepancy for goodness-of-fit tests. In *International conference on machine learning*.

Lyne, A. M., Girolami, M., Atchadé, Y., Strathmann, H., and Simpson, D. (2015). On Russian Roulette estimates for Bayesian inference with doubly-intractable likelihoods. *Statistical Science*, 30(4):443–467.

Metropolis, N., Rosenbluth, A. W., Rosenbluth, M. N., Teller, A. H., and Teller, E. (1953). Equation of state calculations by fast computing machines. *The journal of chemical physics*, 21(6):1087–1092.

Møller, J., Pettitt, A. N., Reeves, R., and Berthelsen, K. K. (2006). An efficient Markov chain Monte Carlo method for distributions with intractable normalising constants. *Biometrika*, 93(2):451–458.

Müller, A. (1997). Integral probability metrics and their generating classes of functions. *Advances in Applied Probability*, 29(2):429–443.

Murray, I., Ghahramani, Z., and Mackay, D. J. C. (2006). MCMC for doubly-intractable distributions. In *Proceedings of the 22nd Annual Conference on Uncertainty in Artificial Intelligence*, pages 359–366.

Park, J. and Haran, M. (2018). Bayesian inference in the presence of intractable normalizing functions. *Journal of the American Statistical Association*, 113(523):1372–1390.

Park, J. and Haran, M. (2020). A function emulation approach for doubly intractable distributions. *Journal of Computational and Graphical Statistics*, 29(1):66–77.

Propp, J. G. and Wilson, D. B. (1996). Exact sampling with coupled Markov chains and applications to statistical mechanics. *Random Structures & Algorithms*, 9(1-2):223–252.

Rao, V., Lin, L., and Dunson, D. B. (2016). Data augmentation for models based on rejection sampling. *Biometrika*, 103:319–335.

Ribeiro, E. E., Zeviani, W. M., Bonat, W. H., Demetrio, C. G., and Hinde, J. (2020). Reparametrization of COM–Poisson regression models with applications in the analysis of experimental data. *Statistical Modelling*, 20:443–466.

Robert, C. and Casella, G. (2013). *Monte Carlo statistical methods*. Springer Science & Business Media, New York.

Robins, G., Pattison, P., Kalish, Y., and Lusher, D. (2007). An introduction to exponential random graph (p\*) models for social networks. *Social Networks*, 29(2):173–191.

Roy, V. (2020). Convergence diagnostics for Markov chain Monte Carlo. *Annual Review of Statistics and Its Application*, 7:387–412.

Sáez-Castillo, A. J. and Conde-Sánchez, A. (2013). A hyper-Poisson regression model for overdispersed and underdispersed count data. *Computational Statistics and Data Analysis*, 61:148–157.

Shmueli, G., Minka, T. P., Kadane, J. B., Borle, S., and Boatwright, P. (2005). A useful distribution for fitting discrete data: Revival of the Conway–Maxwell–Poisson distribution. *Journal of the Royal Statistical Society: Series C*, 54:127–142.

Stein, C. (1972). A bound for the error in the normal approximation to the distribution of a sum of dependent random variables. In *Proceedings of the Sixth Berkeley Symposium on Mathematical Statistics and Probability*, volume 2, pages 583–602.

Strauss, D. J. (1975). A model for clustering. *Biometrika*, 62(2):467–475.

Vats, D., Gonçalves, F., Łatuszyński, K., and Roberts, G. (2022). Efficient Bernoulli factory Markov chain Monte Carlo for intractable posteriors. *Biometrika*, 109:369–385.

Xing, H., Nicholls, G. K., and Lee, J. E. (2019). Calibrated approximate Bayesian inference. In *Proceedings of the 36th International Conference on Machine Learning*, volume 97 of *Proceedings of Machine Learning Research*, pages 6912–6920.

# Supplementary Material for “Diagnostics for Monte Carlo Algorithms for Models with Intractable Normalising Functions”

Bokgyeong Kang, John Hughes, and Murali Haran

## A Proof of Theorem 1

### A.1 Derivative of log normalising function

For a  $p$ -dimensional parameter vector  $\boldsymbol{\theta}$ , consider a posterior density  $\pi(\boldsymbol{\theta} \mid \mathbf{x})$  whose likelihood function is  $L(\boldsymbol{\theta} \mid \mathbf{x}) = h(\mathbf{x} \mid \boldsymbol{\theta})/c(\boldsymbol{\theta})$  and prior density is  $p(\boldsymbol{\theta})$ . The  $k$ th entry of  $\nabla_{\boldsymbol{\theta}} \log c(\boldsymbol{\theta} \mid \mathbf{x})$ , the score function of the normalising function, can be written as

$$\begin{aligned}
 \frac{\partial \log c(\boldsymbol{\theta})}{\partial \theta_k} &= \frac{1}{c(\boldsymbol{\theta})} \frac{\partial c(\boldsymbol{\theta})}{\partial \theta_k} \\
 &= \frac{1}{c(\boldsymbol{\theta})} \frac{\partial}{\partial \theta_k} \int_{\mathbf{x}} h(\mathbf{x} \mid \boldsymbol{\theta}) d\mathbf{x} \\
 &= \frac{1}{c(\boldsymbol{\theta})} \int_{\mathbf{x}} \frac{\partial h(\mathbf{x} \mid \boldsymbol{\theta})}{\partial \theta_k} d\mathbf{x} \\
 &= \frac{1}{c(\boldsymbol{\theta})} \int_{\mathbf{x}} h(\mathbf{x} \mid \boldsymbol{\theta}) \frac{\partial \log h(\mathbf{x} \mid \boldsymbol{\theta})}{\partial \theta_k} d\mathbf{x} \\
 &= \int_{\mathbf{x}} \frac{\partial \log h(\mathbf{x} \mid \boldsymbol{\theta})}{\partial \theta_k} f(\mathbf{x} \mid \boldsymbol{\theta}) d\mathbf{x} \\
 &= \mathbb{E}_f \left\{ \frac{\partial \log h(\mathbf{x} \mid \boldsymbol{\theta})}{\partial \theta_k} \right\}.
 \end{aligned} \tag{1}$$

(2)

Equation (1) follows from the dominated convergence theorem. Under the assumptions that the score function exists and the score function and the normalising function are bounded, we have exchanged the derivative with the integral.

## A.2 Second derivative of log normalising function

The  $(k, l)$ th entry of  $\frac{\partial}{\partial \boldsymbol{\theta}} \nabla_{\boldsymbol{\theta}} \log c(\boldsymbol{\theta} \mid \mathbf{x})$ , the Hessian matrix of the normalising function, is given by

$$\begin{aligned} \frac{\partial^2 \log c(\boldsymbol{\theta})}{\partial \theta_k \partial \theta_l} &= \frac{\partial}{\partial \theta_k} \left\{ \frac{1}{c(\boldsymbol{\theta})} \frac{\partial c(\boldsymbol{\theta})}{\partial \theta_l} \right\} \\ &= \frac{1}{c(\boldsymbol{\theta})} \frac{\partial^2 c(\boldsymbol{\theta})}{\partial \theta_k \partial \theta_l} - \left\{ \frac{1}{c(\boldsymbol{\theta})} \frac{\partial c(\boldsymbol{\theta})}{\partial \theta_k} \right\} \left\{ \frac{1}{c(\boldsymbol{\theta})} \frac{\partial c(\boldsymbol{\theta})}{\partial \theta_l} \right\} \\ &= \frac{1}{c(\boldsymbol{\theta})} \frac{\partial^2 c(\boldsymbol{\theta})}{\partial \theta_k \partial \theta_l} - \mathbb{E}_f \left\{ \frac{\partial \log h(\mathbf{X} \mid \boldsymbol{\theta})}{\partial \theta_k} \right\} \mathbb{E}_f \left\{ \frac{\partial \log h(\mathbf{X} \mid \boldsymbol{\theta})}{\partial \theta_l} \right\}. \end{aligned} \quad (3)$$

Now consider the first term on the right hand side of equation (3). It can be written as

$$\begin{aligned} \frac{1}{c(\boldsymbol{\theta})} \frac{\partial^2 c(\boldsymbol{\theta})}{\partial \theta_k \partial \theta_l} &= \frac{1}{c(\boldsymbol{\theta})} \frac{\partial^2}{\partial \theta_k \partial \theta_l} \int_{\mathbf{x}} h(\mathbf{x} \mid \boldsymbol{\theta}) d\mathbf{x} \\ &= \frac{1}{c(\boldsymbol{\theta})} \int_{\mathbf{x}} \frac{\partial}{\partial \theta_k} \left\{ \frac{\partial \log h(\mathbf{x} \mid \boldsymbol{\theta})}{\partial \theta_l} h(\mathbf{x} \mid \boldsymbol{\theta}) \right\} d\mathbf{x} \end{aligned} \quad (4)$$

$$\begin{aligned} &= \int_{\mathbf{x}} \frac{\partial^2 \log h(\mathbf{x} \mid \boldsymbol{\theta})}{\partial \theta_k \partial \theta_l} f(\mathbf{x} \mid \boldsymbol{\theta}) d\mathbf{x} + \int_{\mathbf{x}} \frac{\partial \log h(\mathbf{x} \mid \boldsymbol{\theta})}{\partial \theta_k} \frac{\partial \log h(\mathbf{x} \mid \boldsymbol{\theta})}{\partial \theta_l} f(\mathbf{x} \mid \boldsymbol{\theta}) d\mathbf{x} \\ &= \mathbb{E}_f \left\{ \frac{\partial^2 \log h(\mathbf{X} \mid \boldsymbol{\theta})}{\partial \theta_k \partial \theta_l} \right\} + \mathbb{E}_f \left\{ \frac{\partial \log h(\mathbf{X} \mid \boldsymbol{\theta})}{\partial \theta_k} \frac{\partial \log h(\mathbf{X} \mid \boldsymbol{\theta})}{\partial \theta_l} \right\}. \end{aligned} \quad (5)$$

In the equation (4) we have exchanged the derivative with the integral, owing to the dominated convergence theorem. Combining (3) and (5), the entry of  $\frac{\partial}{\partial \boldsymbol{\theta}} \nabla_{\boldsymbol{\theta}} \log c(\boldsymbol{\theta} \mid \mathbf{x})$  is

$$\begin{aligned} \frac{\partial^2 \log c(\boldsymbol{\theta})}{\partial \theta_k \partial \theta_l} &= \mathbb{E}_f \left\{ \frac{\partial^2 \log h(\mathbf{X} \mid \boldsymbol{\theta})}{\partial \theta_k \partial \theta_l} \right\} + \mathbb{E}_f \left\{ \frac{\partial \log h(\mathbf{X} \mid \boldsymbol{\theta})}{\partial \theta_k} \frac{\partial \log h(\mathbf{X} \mid \boldsymbol{\theta})}{\partial \theta_l} \right\} \\ &\quad - \mathbb{E}_f \left\{ \frac{\partial \log h(\mathbf{X} \mid \boldsymbol{\theta})}{\partial \theta_k} \right\} \mathbb{E}_f \left\{ \frac{\partial \log h(\mathbf{X} \mid \boldsymbol{\theta})}{\partial \theta_l} \right\}. \end{aligned} \quad (6)$$

## A.3 Approximation error of second-stage approximation to asymptotic covariance matrix

Let  $D(\boldsymbol{\theta}) = J(\boldsymbol{\theta}) + H(\boldsymbol{\theta})$  and  $D_{k,l}(\boldsymbol{\theta})$  be the  $(k, l)$  entry of  $D(\boldsymbol{\theta})$ . Let  $\hat{D}_{k,l}(\boldsymbol{\theta})$  be the approximation, computed using auxiliary variables  $\mathbf{y}^{(1)}, \dots, \mathbf{y}^{(N)}$  generated from the model distribution, to  $D_{k,l}(\boldsymbol{\theta})$ . For all  $k, l, m, s \in \{1, \dots, p\}$ , the difference between an entry of

$V = \text{E}_\pi\{\mathbf{d}(\boldsymbol{\theta})\mathbf{d}(\boldsymbol{\theta})^\top\}$  and its two-state approximation is

$$\begin{aligned}
& \left| \text{E}_\pi\{D_{k,l}(\boldsymbol{\theta})D_{m,s}(\boldsymbol{\theta})\} - \frac{1}{n} \sum_{i=1}^n \hat{D}_{k,l}(\boldsymbol{\theta}^{(i)})\hat{D}_{m,s}(\boldsymbol{\theta}^{(i)}) \right| \\
& \leq \left| \frac{1}{n} \sum_{i=1}^n D_{k,l}(\boldsymbol{\theta}^{(i)})D_{m,s}(\boldsymbol{\theta}^{(i)}) - \text{E}_\pi\{D_{k,l}(\boldsymbol{\theta})D_{m,s}(\boldsymbol{\theta})\} \right| \\
& \quad + \left| \frac{1}{n} \sum_{i=1}^n \left\{ \hat{D}_{k,l}(\boldsymbol{\theta}^{(i)})\hat{D}_{m,s}(\boldsymbol{\theta}^{(i)}) - D_{k,l}(\boldsymbol{\theta}^{(i)})D_{m,s}(\boldsymbol{\theta}^{(i)}) \right\} \right| \\
& \leq \delta(n) + \frac{1}{n} \sum_{i=1}^n \left| \hat{D}_{k,l}(\boldsymbol{\theta}^{(i)})\hat{D}_{m,s}(\boldsymbol{\theta}^{(i)}) - D_{k,l}(\boldsymbol{\theta}^{(i)})D_{m,s}(\boldsymbol{\theta}^{(i)}) \right|, \tag{7}
\end{aligned}$$

where  $\delta(n) = \|\frac{1}{n} \sum_{i=1}^n \mathbf{d}(\boldsymbol{\theta}^{(i)})\mathbf{d}(\boldsymbol{\theta}^{(i)})^\top - \text{E}_\pi\{\mathbf{d}(\boldsymbol{\theta})\mathbf{d}(\boldsymbol{\theta})^\top\}\|_{\max} = \mathcal{O}(1/\sqrt{n})$  from the ergodic theorem. Now we consider the second term on the right hand side of inequality (7). Let  $u_k(\boldsymbol{\theta})$  be the  $k$ th entry of the score function  $\mathbf{u}(\boldsymbol{\theta})$  of the posterior distribution and  $\hat{u}_k(\boldsymbol{\theta})$  be its approximation computed using the auxiliary variables. Let  $H_{k,l}(\boldsymbol{\theta})$  be the  $(k,l)$ th entry of the hessian matrix  $H(\boldsymbol{\theta})$  of the posterior distribution and  $\hat{H}_{k,l}(\boldsymbol{\theta})$  be its approximation computed using the auxiliary variables. We can bound the difference between  $\hat{D}_{k,l}(\boldsymbol{\theta})\hat{D}_{m,s}(\boldsymbol{\theta})$  and  $D_{k,l}(\boldsymbol{\theta})D_{m,s}(\boldsymbol{\theta})$  as follows. For all  $k, l, m, s \in \{1, \dots, p\}$ , we have

$$\begin{aligned}
\left| \hat{D}_{k,l}(\boldsymbol{\theta})\hat{D}_{m,s}(\boldsymbol{\theta}) - D_{k,l}(\boldsymbol{\theta})D_{m,s}(\boldsymbol{\theta}) \right| & \leq |\hat{u}_k(\boldsymbol{\theta})\hat{u}_l(\boldsymbol{\theta})\hat{u}_m(\boldsymbol{\theta})\hat{u}_s(\boldsymbol{\theta}) - u_k(\boldsymbol{\theta})u_l(\boldsymbol{\theta})u_m(\boldsymbol{\theta})u_s(\boldsymbol{\theta})| \\
& \quad + \left| \hat{u}_k(\boldsymbol{\theta})\hat{u}_l(\boldsymbol{\theta})\hat{H}_{m,s}(\boldsymbol{\theta}) - u_k(\boldsymbol{\theta})u_l(\boldsymbol{\theta})H_{m,s}(\boldsymbol{\theta}) \right| \\
& \quad + \left| \hat{u}_m(\boldsymbol{\theta})\hat{u}_s(\boldsymbol{\theta})\hat{H}_{k,l}(\boldsymbol{\theta}) - u_m(\boldsymbol{\theta})u_s(\boldsymbol{\theta})H_{k,l}(\boldsymbol{\theta}) \right| \\
& \quad + \left| \hat{H}_{k,l}(\boldsymbol{\theta})\hat{H}_{m,s}(\boldsymbol{\theta}) - H_{k,l}(\boldsymbol{\theta})H_{m,s}(\boldsymbol{\theta}) \right|. \tag{8}
\end{aligned}$$

Let

$$\begin{aligned}
\epsilon_1(N) &= \max_k \left| \frac{1}{N} \sum_{j=1}^N \frac{\partial \log h(\mathbf{y}^{(j)}|\boldsymbol{\theta})}{\partial \theta_k} - \mathbb{E}_f \left\{ \frac{\partial \log h(\mathbf{X}|\boldsymbol{\theta})}{\partial \theta_k} \right\} \right|, \\
\epsilon_2(N) &= \max_{k,l} \left| \frac{1}{N} \sum_{j=1}^N \frac{\partial^2 \log h(\mathbf{y}^{(j)}|\boldsymbol{\theta})}{\partial \theta_k \partial \theta_l} - \mathbb{E}_f \left\{ \frac{\partial^2 \log h(\mathbf{X}|\boldsymbol{\theta})}{\partial \theta_k \partial \theta_l} \right\} \right|, \\
\epsilon_3(N) &= \max_l \left| \frac{1}{N} \sum_{j=1}^N \frac{\partial^3 \log h(\mathbf{y}^{(j)}|\boldsymbol{\theta})}{\partial \theta_k \partial \theta_l \partial \theta_m} - \mathbb{E}_f \left\{ \frac{\partial^3 \log h(\mathbf{X}|\boldsymbol{\theta})}{\partial \theta_k \partial \theta_l \partial \theta_m} \right\} \right|, \\
\epsilon_4(N) &= \max_{k,l} \left| \frac{1}{N} \sum_{j=1}^N \left\{ \frac{\partial \log h(\mathbf{y}^{(j)}|\boldsymbol{\theta})}{\partial \theta_k} \right\} \left\{ \frac{\partial \log h(\mathbf{y}^{(j)}|\boldsymbol{\theta})}{\partial \theta_l} \right\} - \mathbb{E}_f \left\{ \frac{\partial \log h(\mathbf{X}|\boldsymbol{\theta})}{\partial \theta_k} \frac{\partial \log h(\mathbf{X}|\boldsymbol{\theta})}{\partial \theta_l} \right\} \right|, \\
\epsilon_5(N) &= \max_{k,l,m} \left| \frac{1}{N} \sum_{j=1}^N \left\{ \frac{\partial \log h(\mathbf{y}^{(j)}|\boldsymbol{\theta})}{\partial \theta_k} \right\} \left\{ \frac{\partial^2 \log h(\mathbf{y}^{(j)}|\boldsymbol{\theta})}{\partial \theta_l \partial \theta_m} \right\} - \mathbb{E}_f \left\{ \frac{\partial \log h(\mathbf{X}|\boldsymbol{\theta})}{\partial \theta_k} \frac{\partial^2 \log h(\mathbf{X}|\boldsymbol{\theta})}{\partial \theta_l \partial \theta_m} \right\} \right|, \\
\epsilon_6(N) &= \max_{k,l,m} \left| \frac{1}{N} \sum_{j=1}^N \left\{ \frac{\partial \log h(\mathbf{y}^{(j)}|\boldsymbol{\theta})}{\partial \theta_k} \right\} \left\{ \frac{\partial \log h(\mathbf{y}^{(j)}|\boldsymbol{\theta})}{\partial \theta_l} \right\} \left\{ \frac{\partial \log h(\mathbf{y}^{(j)}|\boldsymbol{\theta})}{\partial \theta_m} \right\} \right. \\
&\quad \left. - \mathbb{E}_f \left\{ \frac{\partial \log h(\mathbf{X}|\boldsymbol{\theta})}{\partial \theta_k} \frac{\partial \log h(\mathbf{X}|\boldsymbol{\theta})}{\partial \theta_l} \frac{\partial \log h(\mathbf{X}|\boldsymbol{\theta})}{\partial \theta_m} \right\} \right|,
\end{aligned}$$

and  $\epsilon(N) = \max \{\epsilon_1(N), \epsilon_2(N), \epsilon_3(N), \epsilon_4(N), \epsilon_5(N), \epsilon_6(N)\} = \mathcal{O}(1/\sqrt{N})$  from the ergodic theorem. Now consider the first term on the right hand side of inequality (8). For all  $k, l, m, s \in \{1, \dots, p\}$ , we have

$$\begin{aligned}
&|\hat{u}_k(\boldsymbol{\theta})\hat{u}_l(\boldsymbol{\theta})\hat{u}_m(\boldsymbol{\theta})\hat{u}_s(\boldsymbol{\theta}) - u_k(\boldsymbol{\theta})u_l(\boldsymbol{\theta})u_m(\boldsymbol{\theta})u_s(\boldsymbol{\theta})| \\
&\leq \{4(c'_p + c'_h)^3 + 12c'_h(c'_p + c'_h)^2 + 12c'^2_h(c'_p + c'_h) + 4c'^3_h\} \epsilon(N),
\end{aligned}$$

which follows from Assumptions 1 and 2, and the following elementary inequalities:

$$\begin{aligned}
|ab - \hat{a}\hat{b}| &= |ab - \hat{a}b + \hat{a}b - \hat{a}\hat{b}| = |(a - \hat{a})b + (b - \hat{b})\hat{a}| \\
&\leq |a - \hat{a}||b| + |b - \hat{b}||\hat{a}|,
\end{aligned} \tag{9}$$

$$\begin{aligned}
|abc - \hat{a}\hat{b}\hat{c}| &= |abc - \hat{a}bc + \hat{a}bc - \hat{a}\hat{b}\hat{c}| = |(a - \hat{a})bc + (bc - \hat{b}\hat{c})\hat{a}| \\
&\leq |a - \hat{a}||b||c| + |bc - \hat{b}\hat{c}||\hat{a}|,
\end{aligned} \tag{10}$$

$$\begin{aligned}
|abcd - \hat{a}\hat{b}\hat{c}\hat{d}| &= |abcd - \hat{a}bcd + \hat{a}bcd - \hat{a}\hat{b}\hat{c}\hat{d}| = |(a - \hat{a})bcd + (bcd - \hat{b}\hat{c}\hat{d})\hat{a}| \\
&\leq |a - \hat{a}||b||c||d| + |bcd - \hat{b}\hat{c}\hat{d}||\hat{a}|.
\end{aligned} \tag{11}$$

Now consider the remaining terms on the right hand side of inequality (8). In a similar fashion, for all  $k, l, m, s \in \{1, \dots, p\}$ , we have

$$\begin{aligned} & \left| \hat{u}_k(\boldsymbol{\theta}) \hat{u}_l(\boldsymbol{\theta}) \hat{H}_{m,s}(\boldsymbol{\theta}) - u_k(\boldsymbol{\theta}) u_l(\boldsymbol{\theta}) H_{m,s}(\boldsymbol{\theta}) \right| \\ & \leq \left\{ (8c'_h + 6c'^2_h)(c'_p + c'_h) + 2(1 + c'_h)(c'_p + c'_h)^2 + (2c'_p + 4c'_h)(c''_p + c''_h) + 6c''_h + 4c'^2_h \right\} \epsilon(N), \\ & \left| \hat{u}_m(\boldsymbol{\theta}) \hat{u}_s(\boldsymbol{\theta}) \hat{H}_{k,l}(\boldsymbol{\theta}) - u_m(\boldsymbol{\theta}) u_s(\boldsymbol{\theta}) H_{k,l}(\boldsymbol{\theta}) \right| \\ & \leq \left\{ (8c'_h + 6c'^2_h)(c'_p + c'_h) + 2(1 + c'_h)(c'_p + c'_h)^2 + (2c'_p + 4c'_h)(c''_p + c''_h) + 6c''_h + 4c'^2_h \right\} \epsilon(N), \end{aligned}$$

and

$$|\hat{H}_{k,l}(\boldsymbol{\theta}) \hat{H}_{m,s}(\boldsymbol{\theta}) - H_{k,l}(\boldsymbol{\theta}) H_{m,s}(\boldsymbol{\theta})| \leq \left\{ 4(c''_p + c''_h) + 4c'_h(c''_p + c''_h) + 8c'_h + 12c'^2_h + 4c'^3_h \right\} \epsilon(N).$$

These inequalities follow from Assumptions 1 and 2 in the manuscript and inequalities (9) to (11). Therefore, the approximation error of the two-stage approximation to the asymptotic covariance matrix is

$$\|\hat{V}_{n,N} - V\|_{\max} \leq \delta(n) + g(c'_p, c'_h, c''_p, c''_h) \epsilon(N),$$

almost surely for some bounded function  $g$ ,  $\delta(n) = \mathcal{O}(1/\sqrt{n})$ , and  $\epsilon(N) = \mathcal{O}(1/\sqrt{N})$ . We use  $\|\cdot\|_{\max}$  to represent the max norm of vectors or matrices.

## B Proof of Theorem 2

Consider a target distribution  $P$  and a weighted sample  $Q_n = \sum_{i=1}^n q_n(\boldsymbol{\theta}^{(i)}) \delta_{\boldsymbol{\theta}^{(i)}}$  targeting  $P$ , where  $\boldsymbol{\theta}^{(1)}, \dots, \boldsymbol{\theta}^{(n)}$  are sample points and  $q_n$  is a probability mass function. By Minkowski's inequality, the difference between IMQ KSD and AIKS of  $Q_n$  is

$$\left| \hat{\mathcal{S}}(Q_n, \mathcal{T}_P, \mathcal{G}_{k, \|\cdot\|_p}) - \mathcal{S}(Q_n, \mathcal{T}_P, \mathcal{G}_{k, \|\cdot\|_p}) \right| \leq \|\hat{\mathbf{w}} - \mathbf{w}\|_p.$$

We now consider the term on the right hand side of this inequality.

$$\begin{aligned}
\|\hat{\mathbf{w}} - \mathbf{w}\|_p^p &= \sum_{j=1}^p |\hat{w}_j - w_j|^p \\
&= \sum_{j=1}^p \frac{|\hat{w}_j - w_j|^{p-1}}{\hat{w}_j + w_j} |\hat{w}_j^2 - w_j^2| \\
&= \sum_{j=1}^p \frac{|\hat{w}_j - w_j|^{p-1}}{\hat{w}_j + w_j} \sum_{k,l=1}^n q_n(\boldsymbol{\theta}^{(k)}) q_n(\boldsymbol{\theta}^{(l)}) \left| \hat{k}_0^j(\boldsymbol{\theta}^{(k)}, \boldsymbol{\theta}^{(l)}) - k_0^j(\boldsymbol{\theta}^{(k)}, \boldsymbol{\theta}^{(l)}) \right|.
\end{aligned}$$

Let  $\epsilon(N) = \max_k \|\hat{\mathbf{u}}(\boldsymbol{\theta}^{(k)}) - \mathbf{u}(\boldsymbol{\theta}^{(k)})\|_{\max} = \mathcal{O}(1/\sqrt{N})$  from ergodic theorem. The approximate error for the Stein kernel can be derived as follows.

$$\begin{aligned}
&\left| \hat{k}_0^j(\boldsymbol{\theta}^{(k)}, \boldsymbol{\theta}^{(l)}) - k_0^j(\boldsymbol{\theta}^{(k)}, \boldsymbol{\theta}^{(l)}) \right| \\
&\leq k(\boldsymbol{\theta}^{(k)}, \boldsymbol{\theta}^{(l)}) \left| \hat{u}_j(\boldsymbol{\theta}^{(k)}) \hat{u}_j(\boldsymbol{\theta}^{(l)}) - u_j(\boldsymbol{\theta}^{(k)}) u_j(\boldsymbol{\theta}^{(l)}) \right| \\
&+ \left| \nabla_{\theta_j^{(l)}} k(\boldsymbol{\theta}^{(k)}, \boldsymbol{\theta}^{(l)}) \right| \left| \hat{u}_j(\boldsymbol{\theta}^{(k)}) - u_j(\boldsymbol{\theta}^{(k)}) \right| \\
&+ \left| \nabla_{\theta_j^{(k)}} k(\boldsymbol{\theta}^{(l)}, \boldsymbol{\theta}^{(k)}) \right| \left| \hat{u}_j(\boldsymbol{\theta}^{(l)}) - u_j(\boldsymbol{\theta}^{(l)}) \right| \\
&\leq \left[ k(\boldsymbol{\theta}^{(k)}, \boldsymbol{\theta}^{(l)}) \left\{ |\hat{u}_j(\boldsymbol{\theta}^{(k)})| + |u_j(\boldsymbol{\theta}^{(l)})| \right\} + 2 |\nabla_{\theta_j^{(l)}} k(\boldsymbol{\theta}^{(k)}, \boldsymbol{\theta}^{(l)})| \right] \epsilon(N) \quad (12) \\
&\leq c_1 \epsilon(N)
\end{aligned}$$

for bounded constant  $c_1$ . The inequality in (12) follows from (9) and the fact that  $\nabla_{\theta_j^{(l)}} k(\boldsymbol{\theta}^{(k)}, \boldsymbol{\theta}^{(l)})$  and  $\nabla_{\theta_j^{(k)}} k(\boldsymbol{\theta}^{(l)}, \boldsymbol{\theta}^{(k)})$  are symmetric around zero. Now,

$$\begin{aligned}
\|\hat{\mathbf{w}} - \mathbf{w}\|_p^p &\leq c_1 \epsilon(N) \sum_{j=1}^p \frac{|\hat{w}_j - w_j|^{p-1}}{\hat{w}_j + w_j} \sum_{k,l=1}^n q_n(\boldsymbol{\theta}^{(k)}) q_n(\boldsymbol{\theta}^{(l)}) \\
&\leq n^2 c_1 c_2 \epsilon(N)
\end{aligned}$$

for bounded constant  $c_2$ . Therefore, the approximate error for AIKS is

$$\left| \hat{\mathcal{S}}(Q_n, \mathcal{T}_P, \mathcal{G}_{k, \|\cdot\|_p}) - \mathcal{S}(Q_n, \mathcal{T}_P, \mathcal{G}_{k, \|\cdot\|_p}) \right| \leq [n^2 M \epsilon(N)]^{1/p}$$

almost surely for some bounded constant  $M$  and  $\epsilon(N) = \mathcal{O}(1/\sqrt{N})$ .

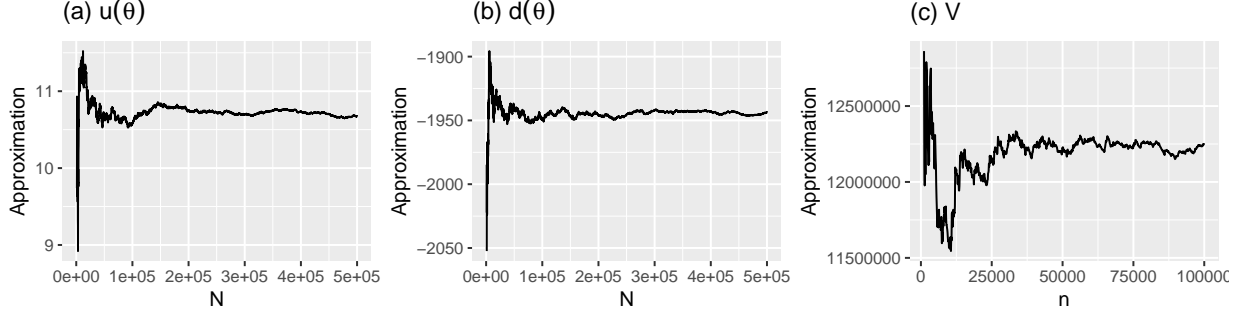


Figure 1: Results from the Ising model for the simulated lattice. (a) Approximation  $\hat{u}_N(\theta)$  to the score function against the auxiliary sample size  $N$ , given a fixed value of  $\theta$ . (b) Approximation  $\hat{d}_N(\theta)$  to the distance between  $H(\theta)$  and  $J(\theta)$  against the auxiliary sample size  $N$ , given the fixed value of  $\theta$ . (c) Approximation  $\hat{V}_{n,N}$  to the asymptotic variance of  $d(\theta)$  against the posterior sample size  $n$ , given  $N = 200,000$ .

## C Choice of tuning parameters for diagnostics

In this section, we show how we choose the auxiliary sample size  $N$  and posterior sample size  $n$  for our diagnostics in all examples of our manuscript.

### C.1 The Ising model

Figure 1 (a) shows how the approximation  $\hat{u}_N(\theta)$  to the score function  $u(\theta)$  changes with an increasing size  $N$  of auxiliary samples. The approximation appears to have stabilised around  $N$  of 200,000. In Figure 1 (b), it is also observed that the approximation  $\hat{d}_N(\theta)$  to  $d(\theta) = H(\theta) + J(\theta)$  stabilises around  $N$  of 200,000. Thus we choose  $N = 200,000$  for ACD and AIKS. For a long enough posterior sample path, we approximate  $d(\theta^{(i)})$  for  $i = 1, 2, \dots$  for  $N = 200,000$ . Figure 1 (c) shows the approximation  $\hat{V}_{n,N}$  to the asymptotic variance  $V$  against the posterior sample size  $n$ . We observe that the approximation appears to have stabilised around  $n$  of 50,000. Therefore, we choose  $n = 50,000$ .

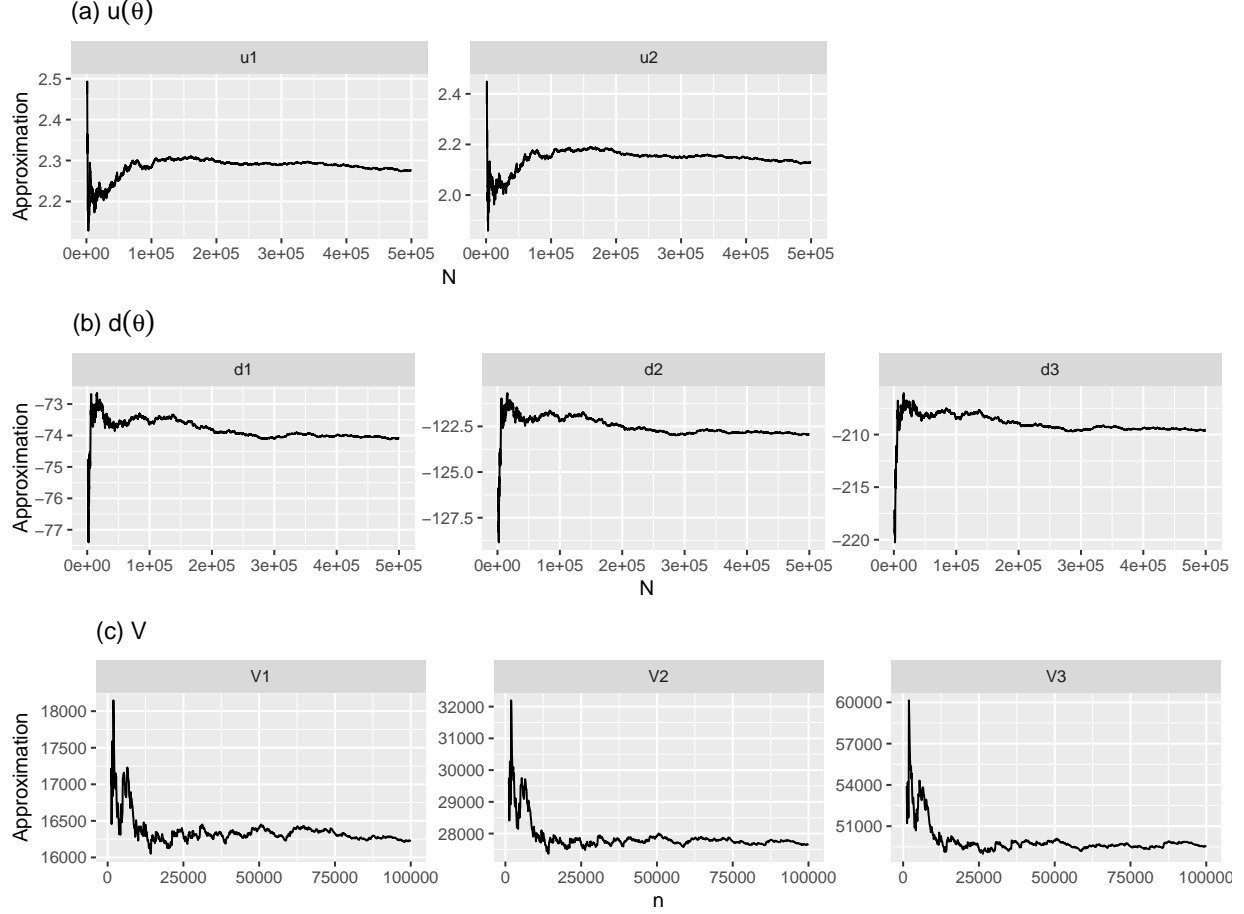


Figure 2: Results from ERGM for the simulated network. (a) Approximation  $\hat{u}_N(\boldsymbol{\theta})$  to the score function  $\hat{\mathbf{u}}(\boldsymbol{\theta})$  against the auxiliary sample size  $N$ , given a fixed value of  $\boldsymbol{\theta}$ . (b) Approximation  $\hat{\mathbf{d}}_N(\boldsymbol{\theta})$  to  $\mathbf{d}(\boldsymbol{\theta})$  against the auxiliary sample size  $N$ , given the fixed value of  $\boldsymbol{\theta}$ . (c) Approximation  $\hat{V}_{n,N}$  to the asymptotic variance  $V$  against the posterior sample size  $n$ , given  $N = 200,000$ .

## C.2 A social network model

Figure 2 (a) shows how the approximation  $\hat{u}_N(\boldsymbol{\theta})$  to the score function  $\mathbf{u}(\boldsymbol{\theta})$  changes with an increasing size  $N$  of auxiliary samples. The approximation appears to have stabilised around  $N$  of 200,000. In Figure 2 (b), it is also observed that the approximation  $\hat{\mathbf{d}}_N(\boldsymbol{\theta})$  to  $\mathbf{d}(\boldsymbol{\theta}) = \text{vech}[H(\boldsymbol{\theta}) + J(\boldsymbol{\theta})]$  stabilises around  $N$  of 200,000. Thus we choose  $N = 200,000$  for ACD and AIKS. For a long enough posterior sample path, we approximate  $\mathbf{d}(\boldsymbol{\theta}^{(i)})$  for

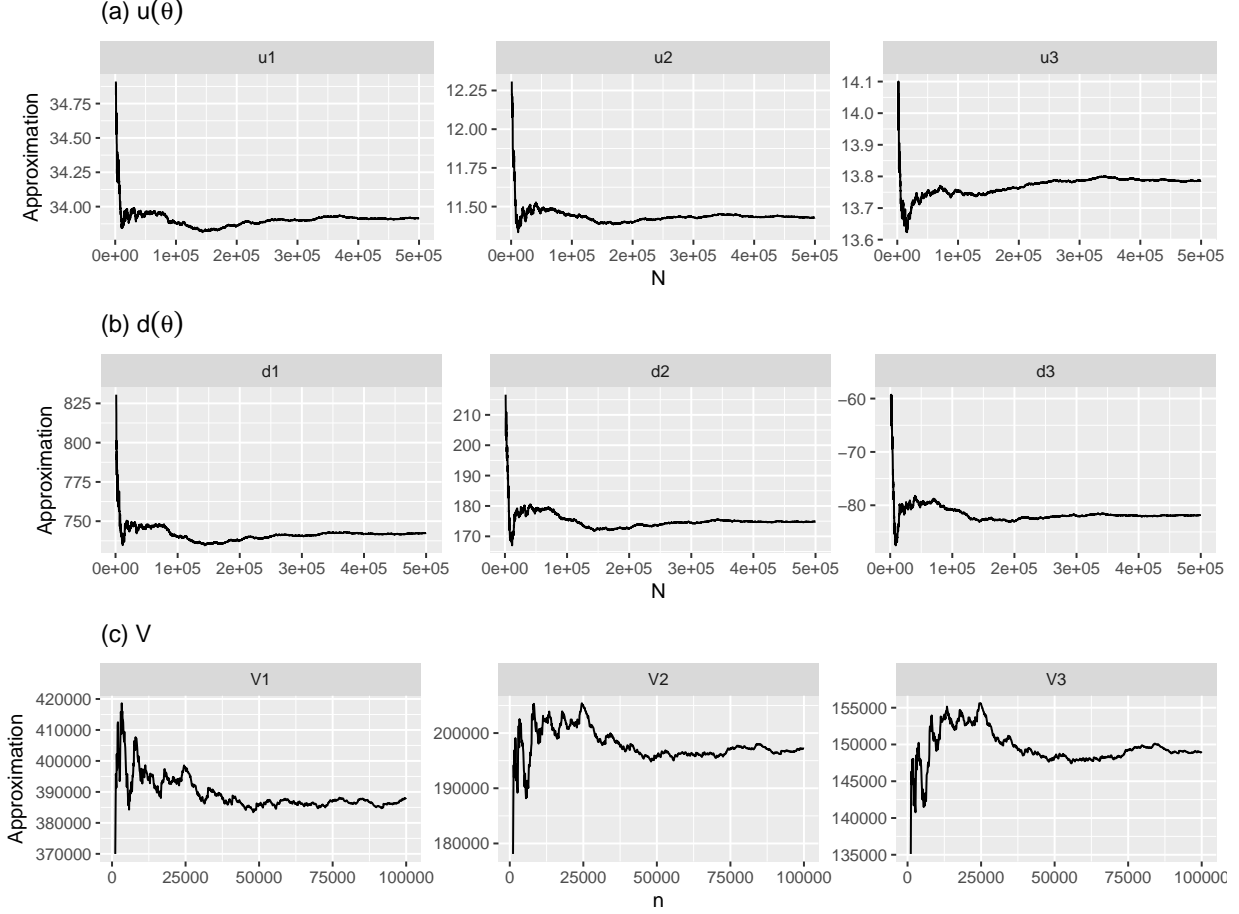


Figure 3: Results from the Conway–Maxwell–Poisson regression model for the takeover bids dataset. (a) Approximation  $\hat{\mathbf{u}}_N(\boldsymbol{\theta})$  to the score function  $\hat{\mathbf{u}}(\boldsymbol{\theta})$  against the auxiliary sample size  $N$ , given a fixed value of  $\boldsymbol{\theta}$ . (b) Approximation  $\hat{\mathbf{d}}_N(\boldsymbol{\theta})$  to  $\mathbf{d}(\boldsymbol{\theta})$  against the auxiliary sample size  $N$ , given the fixed value of  $\boldsymbol{\theta}$ . (c) Approximation  $\hat{V}_{n,N}$  to the asymptotic variance  $V$  against the posterior sample size  $n$ , given  $N = 200,000$ .

$i = 1, 2, \dots$  for  $N = 200,000$ . Figure 2 (c) shows the approximation  $\hat{V}_{n,N}$  to the asymptotic variance  $V$  against the posterior sample size  $n$ . We observe that the approximation appears to have stabilised around  $n$  of 75,000. Therefore, we choose  $n = 75,000$ .

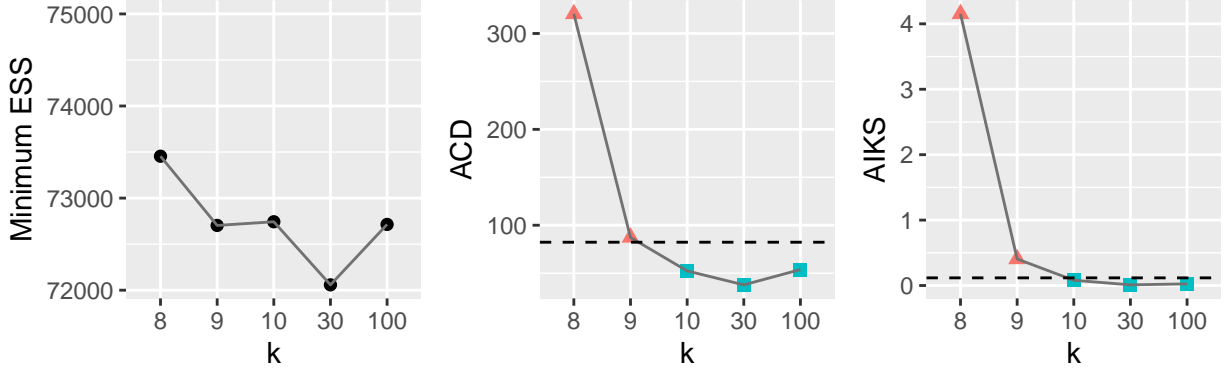


Figure 4: Diagnostics (minimum ESS, ACD, and AIKS) for NormTrunc samples of length  $n = 75,000$  for different levels  $k$  of truncation.

### C.3 A Conway–Maxwell–Poisson regression model

Note that we only provide results regarding the first three elements of a vector or matrix because similar results are observed for the other elements. Figure 3 (a) shows how the approximation  $\hat{\mathbf{u}}_N(\boldsymbol{\theta})$  to the score function  $\mathbf{u}(\boldsymbol{\theta})$  changes with an increasing size  $N$  of auxiliary samples. The approximation appears to have stabilised around  $N$  of 200,000. In Figure 3 (b), it is also observed that the approximation  $\hat{\mathbf{d}}_N(\boldsymbol{\theta})$  to  $\mathbf{d}(\boldsymbol{\theta}) = \text{vech}[H(\boldsymbol{\theta}) + J(\boldsymbol{\theta})]$  stabilises around  $N$  of 200,000. Thus we choose  $N = 200,000$  for ACD and AIKS. For a long enough posterior sample path, we approximate  $\mathbf{d}(\boldsymbol{\theta}^{(i)})$  for  $i = 1, 2, \dots$  for  $N = 200,000$ . Figure 3 (c) shows the approximation  $\hat{V}_{n,N}$  to the asymptotic variance  $V$  against the posterior sample size  $n$ . We observe that the approximation appears to have stabilised around  $n$  of 75,000. In the manuscript, we choose  $n = 100,000$  to show the computing time of a long posterior sample path. Figure 4 shows diagnostics from  $n = 75,000$ , the conclusion of which is consistent with that from  $n = 100,000$  in the manuscript.